Essential Role of the Histone Methyltransferase G9a in Cocaine-Induced Plasticity

Ian Maze, *et al.*

Science **327**, 213 (2010);
DOI: 10.1126/science.1179438

differentiated state. However, these differentiating cells were Pdm1-negative, suggesting that other signals that repress differentiation are present. In accordance with the *dpp* RNAi results, loss-of-function MARCM clones of a Dpp receptor, *thickveins* (*tkv*) (*26*), and a downstream effector molecule, mothers against decapentaplegic (Mad) (*27*), both resulted in premature differentiation of AMPs into large, polyploid, enterocyte-like cells (Fig. 4, C and D) compared with wild-type (WT) MARCM clones (fig. S9).

Our studies suggest how stem cells might be determined during intestinal organogenesis (fig. S10). After symmetric divisions and dispersal during early larval development, a founder AMP undergoes an asymmetric division and signals via the Notch pathway to direct its first daughter to become a PC that acts as a niche, where the AMP and its subsequent daughters can remain undifferentiated in response to a Dpp signal from the PC, and proliferate to form AMP islands. During metamorphosis, the PC breaks down, allowing AMPs in the island to respond to Notch signaling and differentiate into enterocytes. However, one AMP per island, on average, remains undifferentiated and becomes a future ISC. The mechanism that allows this AMP to stay undifferentiated remains to be determined.

Unlike other characterized niches, where a stem or progenitor cell moves away from its niche to differentiate (*1*, *7*, *28*), the PC niche is a holding pen, which does not allow its cells to escape or to differentiate until the niche breaks down. The transition to a functionally homeostatic adult niche that maintains ISCs would require a separate step. Our observations indicate a paradigm that other stem cell systems may also use: The progenitor cell divides to form both niche and stem cells. Such a mechanism that lends greater autonomy to stem cells might exist in other epithelial cell populations during development or tissue homeostasis.

References and Notes

1. T. Xie, A. C. Spradling, *Science* **290**, 328 (2000).
2. A. A. Kiger, D. L. Jones, C. Schulz, M. B. Rogers, M. T. Fuller, *Science* **294**, 2542 (2001).
3. N. Tulina, E. Matunis, *Science* **294**, 2546 (2001).
4. J. Zhang *et al.*, *Nature* **425**, 836 (2003).
5. O. H. Yilmaz, M. J. Kiel, S. J. Morrison, *Blood* **107**, 924 (2006).
6. L. M. Calvi *et al.*, *Nature* **425**, 841 (2003).
7. T. Tumbar *et al.*, *Science* **303**, 359 (2004); published online 11 December 2003 (10.1126/science.1092436).
8. F. Doetsch, *Curr. Opin. Genet. Dev.* **13**, 543 (2003).
9. R. Schofield, *Blood Cells* **4**, 7 (1978).
10. B. Ohlstein, T. Kai, E. Decotto, A. Spradling, *Curr. Opin. Cell Biol.* **16**, 693 (2004).
11. B. Ohlstein, A. Spradling, *Nature* **439**, 470 (2006).
12. C. A. Micchelli, N. Perrimon, *Nature* **439**, 475 (2006).
13. V. J. Hartenstein, Y. N. Jan, *Rouxs Arch. Dev. Biol.* **201**, 194 (1992).
14. H. Jiang, B. A. Edgar, *Development* **136**, 483 (2009).
15. B. Ohlstein, A. Spradling, *Science* **315**, 988 (2007).
16. Materials and methods are available as supporting material on *Science* Online.
17. H. H. El Shatoury, C. H. Waddington, *J. Embryol. Exp. Morphol.* **5**, 9 (1957).
18. L. Nicholson *et al.*, *Genetics* **178**, 215 (2008).
19. C. W. Robertson, *J. Morphol.* **59**, 351 (1936).
20. W. C. Lee, K. Beebe, L. Sudmeier, C. A. Micchelli, *Development* **136**, 2255 (2009).
21. E. A. Bach *et al.*, *Gene Expr. Patterns* **7**, 323 (2007).
22. A. Chitnis, *Dev. Dyn.* **235**, 886 (2006).
23. A. A. Shivdasani, P. W. Ingham, *Curr. Biol.* **13**, 2065 (2003).
24. T. Xie, A. C. Spradling, *Cell* **94**, 251 (1998).
25. E. Kawase, M. D. Wong, B. C. Ding, T. Xie, *Development* **131**, 1365 (2004).
26. T. J. Brummel *et al.*, *Cell* **78**, 251 (1994).
27. J. J. Sekelsky, S. J. Newfeld, L. A. Raftery, E. H. Chartoff, W. M. Gelbart, *Genetics* **139**, 1347 (1995).
28. Y. M. Yamashita, D. L. Jones, M. T. Fuller, *Science* **301**, 1547 (2003).

29. We thank J. Wolken and S. Selway for technical assistance with the Pswitch screen; members of the *Drosophila* community for sending fly stocks; Developmental Studies Hybridoma Bank for antibodies; E. Matunis, M. Buszczak, and J. Wilhelm for helpful discussions; and anonymous reviewers for comments. B.O. is the recipient of the 2009 Searle Scholars Award, the Charles Bohmfalk Research Award, and an NIH grant (R01 DK082456-01).

Supporting Online Material

www.sciencemag.org/cgi/content/full/327/5962/210/DC1
Materials and Methods
Figs. S1 to S10
Table S1
References

15 September 2009; accepted 25 November 2009
10.1126/science.1181958

Essential Role of the Histone Methyltransferase G9a in Cocaine-Induced Plasticity

Ian Maze,[1] Herbert E. Covington III,[1] David M. Dietz,[1] Quincey LaPlant,[1,2] William Renthal,[2] Scott J. Russo,[1] Max Mechanic,[2] Ezekiell Mouzon,[1] Rachael L. Neve,[3] Stephen J. Haggarty,[4,5] Yanhua Ren,[1] Srihari C. Sampath,[6] Yasmin L. Hurd,[1] Paul Greengard,[7] Alexander Tarakhovsky,[6] Anne Schaefer,[7] Eric J. Nestler[1]*

Cocaine-induced alterations in gene expression cause changes in neuronal morphology and behavior that may underlie cocaine addiction. In mice, we identified an essential role for histone 3 lysine 9 (H3K9) dimethylation and the lysine dimethyltransferase G9a in cocaine-induced structural and behavioral plasticity. Repeated cocaine administration reduced global levels of H3K9 dimethylation in the nucleus accumbens. This reduction in histone methylation was mediated through the repression of G9a in this brain region, which was regulated by the cocaine-induced transcription factor ΔFosB. Using conditional mutagenesis and viral-mediated gene transfer, we found that G9a down-regulation increased the dendritic spine plasticity of nucleus accumbens neurons and enhanced the preference for cocaine, thereby establishing a crucial role for histone methylation in the long-term actions of cocaine.

Repeated cocaine exposure is characterized by persistent changes in gene expression and altered neuronal morphology within the rodent nucleus accumbens (NAc), a key component of the brain's reward circuitry (*1*, *2*). Chromatin remodeling is important in aberrant transcriptional changes in this brain region that may underlie aspects of cocaine addiction (*3*–*9*). Cocaine regulation of chromatin structure in the NAc results, in part, from direct cocaine-induced modifications of the chromatin enzymatic machinery, leading to changes in histone acetylation and phosphorylation (*4*, *7*–*9*); however, roles for enzymes controlling histone methylation have not yet been investigated.

A recent genome-wide promoter analysis using chromatin immunoprecipitation coupled to microarrays (ChIP-Chip) identified altered patterns of repressive histone H3 lysine 9 (H3K9) and 27 (H3K27) methylation at specific gene promoters in the NAc after repeated cocaine treatment (*6*). In mice, we therefore profiled numerous lysine methyltransferases (KMTs) and demethylases (KDMs) that are known to control H3K9 or H3K27 methylation (Fig. 1A). Only two enzymes, G9a and G9a-like protein (GLP), displayed persistent transcriptional regulation 24 hours after repeated cocaine administration, when the expression of both genes was significantly down-regulated. Because G9a and GLP specifically catalyze the dimethylation of H3K9 (H3K9me2), their down-regulation by cocaine is consistent with decreased global levels of euchromatic H3K9me2 observed at this time point (Fig. 1B). In contrast, global levels of heterochromatic H3K27 meth-

[1]Fishberg Department of Neuroscience, Mount Sinai School of Medicine, New York, NY, USA. [2]Departments of Psychiatry and Neuroscience, University of Texas Southwestern Medical Center, Dallas, TX, USA. [3]Department of Brain and Cognitive Sciences, Massachusetts Institute of Technology, Cambridge, MA, USA. [4]Psychiatric and Neurodevelopmental Genetics Unit and Molecular Neurogenetics Unit, Center for Human Genetic Research, Massachusetts General Hospital, Boston, MA, USA. [5]Stanley Center for Psychiatric Research, Broad Institute of Harvard and Massachusetts Institute of Technology, Cambridge, MA, USA. [6]Laboratory of Lymphocyte Signaling, The Rockefeller University, New York, NY, USA. [7]Laboratory of Molecular and Cellular Neuroscience, The Rockefeller University, New York, NY, USA.

*To whom correspondence should be addressed. E-mail: eric.nestler@mssm.edu

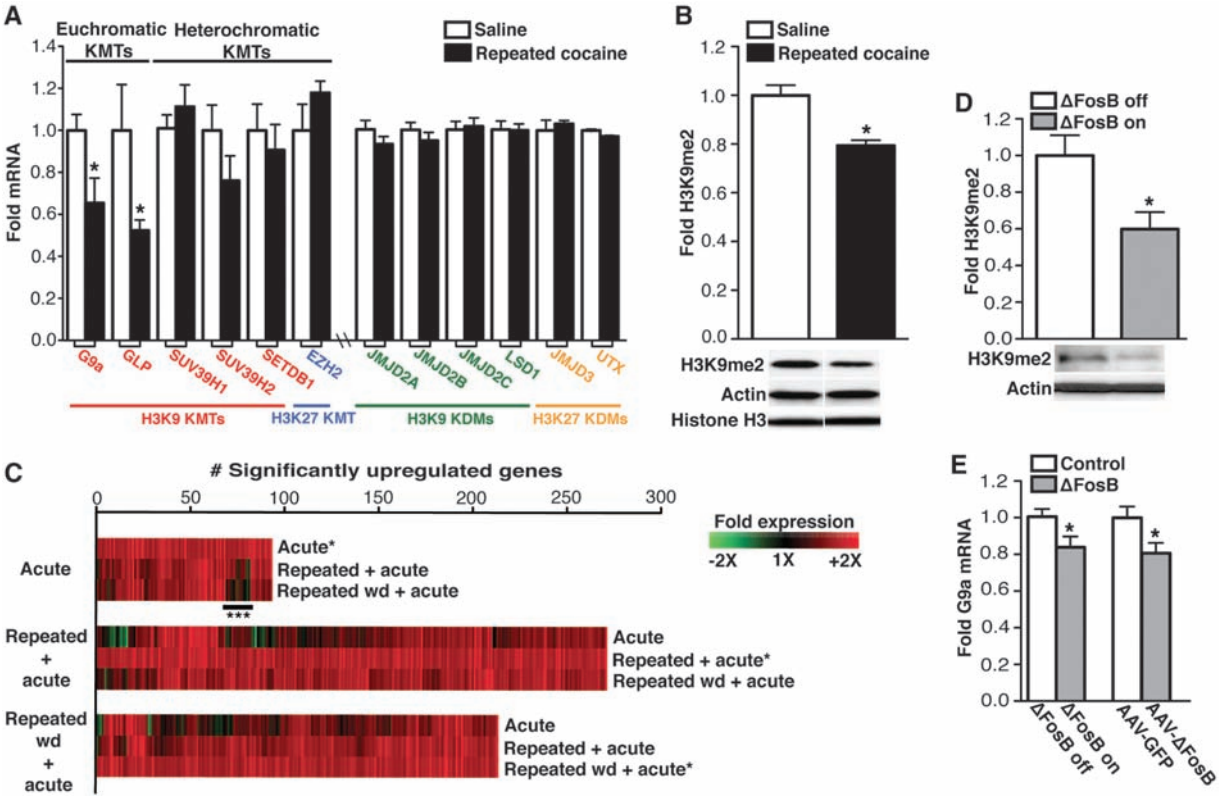

Fig. 1. Repeated cocaine administration represses G9a expression in the NAc through a ΔFosB-dependent mechanism. (**A**) mRNA expression of H3K9/K27 KMTs and KDMs in the NAc 24 hours after repeated cocaine. (**B**) H3K9me2 levels in NAc 24 hours after repeated cocaine. (**C**) Analysis of gene expression after acute or repeated cocaine. Heat maps (*) show genes up-regulated in NAc 1 hour after a cocaine challenge in naïve animals (acute), in animals treated repeatedly with cocaine (repeated + acute), or in animals after 168 hours of withdrawal from repeated cocaine (repeated wd + acute). Associated heat maps show how genes were affected under the other two conditions. Desensitized transcriptional responses after repeated cocaine are indicated (***). (**D**) H3K9me2 levels in the NAc from NSE-*tTA* x tetOP-*ΔFosB* mice on (ΔFosB off) or off (ΔFosB on) doxycycline 1 hour after repeated cocaine. (**E**) G9a mRNA expression in the NAc from NSE-*tTA* x tetOP-*ΔFosB* mice on (ΔFosB off) and off (ΔFosB on) doxycycline and from mice infected with AAV-GFP or AAV-ΔFosB. Data are presented as mean ± SEM. For statistical analyses, see the full figure legends in the supporting online text.

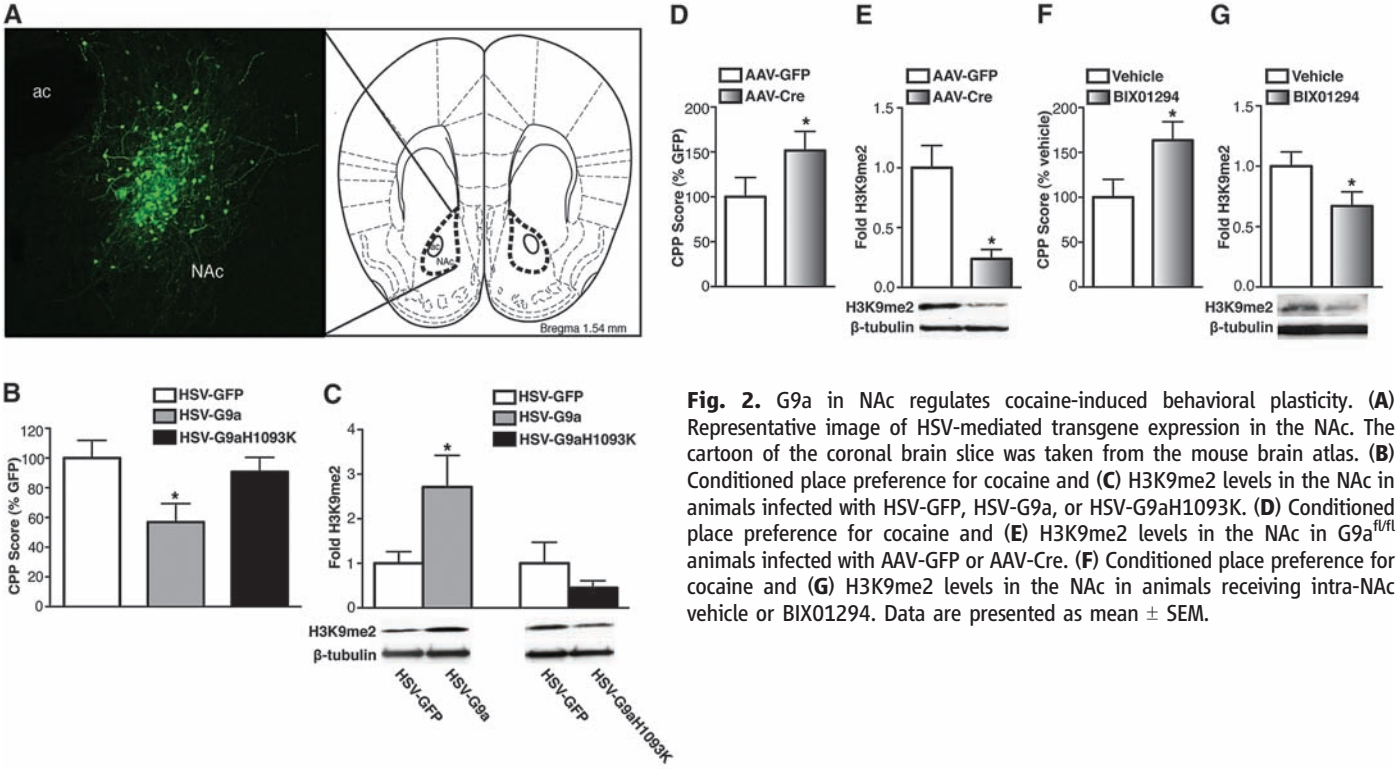

Fig. 2. G9a in NAc regulates cocaine-induced behavioral plasticity. (**A**) Representative image of HSV-mediated transgene expression in the NAc. The cartoon of the coronal brain slice was taken from the mouse brain atlas. (**B**) Conditioned place preference for cocaine and (**C**) H3K9me2 levels in the NAc in animals infected with HSV-GFP, HSV-G9a, or HSV-G9aH1093K. (**D**) Conditioned place preference for cocaine and (**E**) H3K9me2 levels in the NAc in G9a$^{fl/fl}$ animals infected with AAV-GFP or AAV-Cre. (**F**) Conditioned place preference for cocaine and (**G**) H3K9me2 levels in the NAc in animals receiving intra-NAc vehicle or BIX01294. Data are presented as mean ± SEM.

ylation remained unaltered by repeated cocaine exposure (fig. S1). Because of its high levels of catalytic activity both in vitro and in vivo (*10*), we set out to further investigate the functional significance of G9a repression after repeated cocaine exposure in the NAc. Levels of G9a protein, like levels of its mRNA, were significantly reduced 24 hours after repeated cocaine administration (fig. S2). Although G9a mRNA expression was reduced by 35% in the NAc, immunohistochemical analysis revealed a more modest 15% reduction in G9a protein levels, which is consistent with the observed 21% decrease in H3K9me2 after repeated cocaine administration (Fig. 1B). G9a mRNA expression was also down-regulated in this brain region by 20% after repeated self-administration of cocaine (fig. S3).

To identify whether changes in euchromatic H3K9me2 correlate with genome-wide alterations in gene expression in the NAc, we employed microarray analyses to examine gene expression profiles induced by a challenge dose of cocaine in mice with or without a history of prior cocaine exposure (see the gene lists in tables S1 to S3). Animals that had received repeated cocaine displayed dramatically increased gene expression 1 hour after a cocaine challenge, in comparison to acutely treated animals (Fig. 1C). This increased gene expression still occurred in response to a cocaine challenge given after 1 week of withdrawal from repeated cocaine. Consistent with previous reports, a small percentage of genes (~10%) displayed desensitized transcriptional responses after repeated cocaine administration (Fig. 1C and table S1) (*5*). To directly investigate the role of G9a down-regulation in the enhanced gene expression observed after repeated cocaine exposure, mice received intra-NAc injections of herpes simplex virus (HSV) vectors expressing either green fluorescent protein (GFP) or G9a and were treated with saline or repeated cocaine to determine whether G9a overexpression was sufficient to block the repeated cocaine–induced enhancement of gene expression. From a set of 12 randomly selected genes displaying heightened levels of expression after repeated cocaine, we observed that G9a significantly reduced the enhanced expression of 50% of these genes (table S4).

To identify upstream transcriptional events that mediate the repeated cocaine–induced repression of G9a expression, we investigated a possible role for ΔFosB, a highly stable splice product of the immediate early gene *fosB*. ΔFosB accumulates in the NAc after repeated exposure to cocaine, where it has been linked to increased cocaine reward (*11*). ΔFosB can act as either a transcriptional activator or repressor, depending on the target gene involved (*3*, *5*, *6*, *12*). Using bi-transgenic NSE-*tTA* x tetOP-Δ*FosB* mice, wherein ΔFosB expression can be induced selectively in the NAc and dorsal striatum of adult animals (*13*), we examined the impact of ΔFosB expression on cocaine regulation of H3K9me2 and KMTs in the NAc. ΔFosB overexpression was sufficient to reduce levels of both H3K9me2 (Fig. 1D) and G9a expression (Fig. 1E), thereby mimicking the effects of repeated cocaine. In contrast, ΔFosB did not reduce GLP expression in this brain region and had no effect on SUV39H1 and EZH2, the principal trimethylating enzymes for H3K9 and H3K27, respectively (fig. S4). To confirm these data using an independent ΔFosB overexpression system, wild-type adult mice received bilateral intra-NAc injections of adenoassociated virus (AAV) vectors expressing either GFP or ΔFosB. Viral-mediated overexpression of ΔFosB decreased levels of G9a expression in this brain region (Fig. 1E).

Such pronounced and specific regulation of G9a prompted us to investigate whether altering G9a expression specifically in NAc neurons regulates behavioral responses to cocaine. Wild-type mice received intra-NAc injections of HSV vectors expressing GFP or G9a and were then analyzed with an unbiased cocaine-conditioned place-preference paradigm, which provides an indirect measure of drug reward. Viral overexpression of G9a in NAc neurons was con-

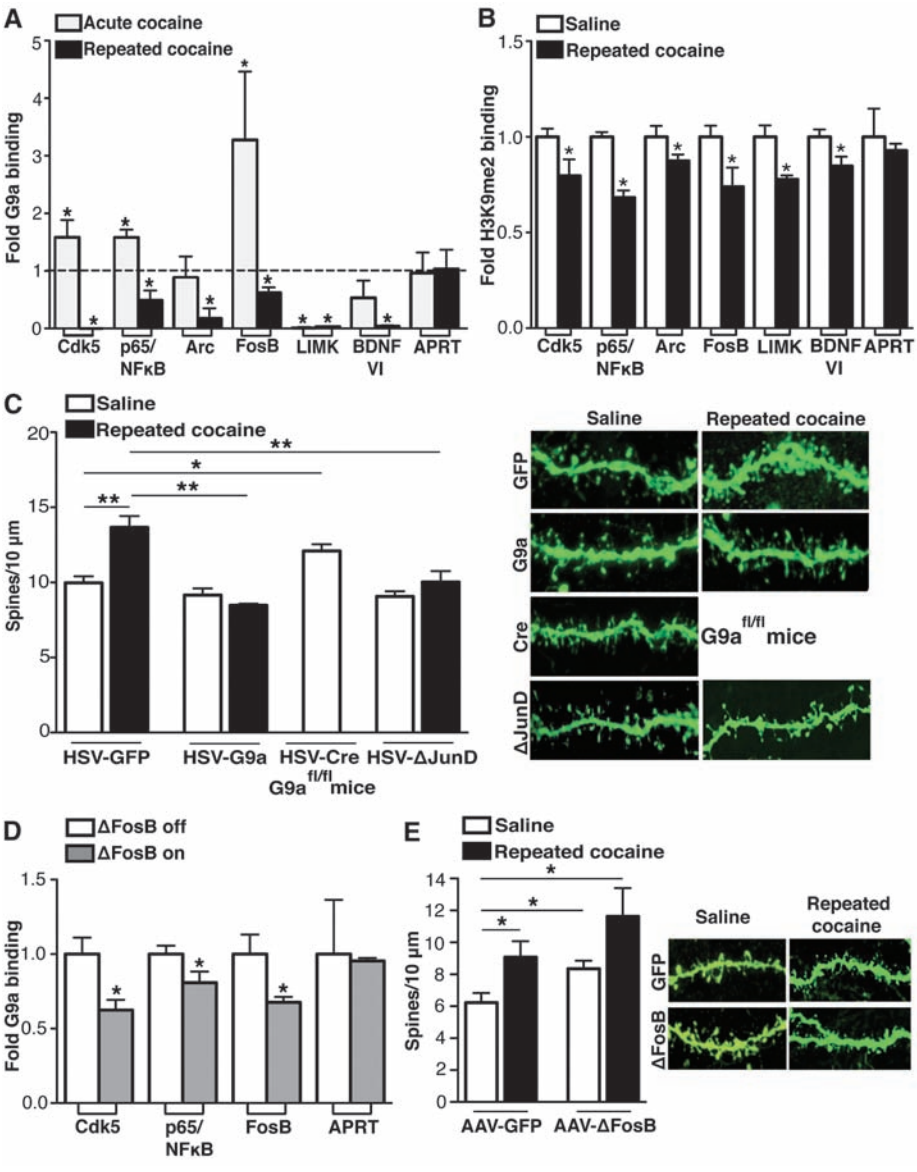

Fig. 3. G9a in the NAc regulates cocaine-induced dendritic spine plasticity. (**A**) Quantitative G9a ChIP in the NAc from animals treated acutely or repeatedly with cocaine, at 1 or 24 hours, respectively. Adenine phosphoribosyltransferase (APRT) was used as a negative control. Data are presented as the relative fold difference from saline controls. (**B**) Quantitative H3K9me2 ChIP in the NAc from repeated cocaine–treated animals at 24 hours, presented as the relative fold difference from saline controls. (**C**) Dendritic spine analysis of animals infected with HSV-GFP, HSV-G9a, or HSV-ΔJunD after repeated cocaine, and dendritic spines in G9a$^{fl/fl}$ mice after HSV-Cre infection. (**D**) Quantitative G9a ChIP in the NAc from NSE-*tTA* x tetOP-Δ*FosB* mice on (ΔFosB off) and off (ΔFosB on) doxycycline. (**E**) Dendritic spine analysis in animals infected with AAV-GFP or AAV-ΔFosB after repeated cocaine. Data are presented as mean ± SEM.

firmed after behavioral testing (Fig. 2A). G9a overexpression significantly decreased the preference for cocaine in comparison to that seen in animals overexpressing GFP (Fig. 2B) and increased H3K9me2 levels in the NAc (Fig. 2C). Overexpression of a catalytically dead mutant of G9a (G9aH1093K) (*14*) did not affect cocaine preference (Fig. 2B) and had no effect on H3K9me2 levels in this brain region (Fig. 2C).

To further study the role of G9a in the behavioral effects of cocaine, and more specifically to mimic the repeated cocaine–induced repression of G9a expression in the NAc, adult $G9a^{fl/fl}$ mice (*14*) received intra-NAc injections of AAV vectors expressing Cre recombinase or GFP as a control. AAV-Cre knockdown of G9a in the NAc, which was confirmed immunohistochemically (fig. S5), significantly increased the effects of cocaine in place-conditioning experiments and decreased H3K9me2 levels in the NAc (Fig. 2, D and E). A commercially available pharmacological inhibitor of G9a and GLP, BIX01294 (*15*, *16*), was used to ascertain whether enzyme inhibition similarly affects behavioral responses to cocaine. Indeed, pharmacological inhibition of G9a and GLP significantly increased the preference for cocaine and decreased H3K9me2 in the NAc (Fig. 2, F and G).

Repeated administration of cocaine increases the density of dendritic spines on NAc medium spiny neurons (*17*), a process associated with functional changes at excitatory glutamatergic synapses onto these neurons (*18*, *19*) and sensitized behavioral responses to the drug (*17*, *20*). We thus hypothesized that down-regulation of G9a activity in the NAc by repeated cocaine exposure might mediate cocaine's ability to regulate the dendritic spine density of NAc neurons. Using ChIP with an antibody to G9a, we identified several putative G9a gene targets in the NAc, each of which has previously been implicated in cocaine-induced dendritic plasticity (Fig. 3A) (*20*–*26*). We found that repeated cocaine administration significantly decreased G9a binding, as well as levels of H3K9me2, at these gene promoters (Fig. 3B). In contrast, acute cocaine administration rapidly recruited G9a to some of these same gene promoters, which is consistent with increased G9a expression observed in the NAc 1 hour after an acute dose of cocaine (fig. S6). Although G9a binding at specific gene promoters correlates with changes in its expression, it remains unclear whether such events are mediated by altered global levels of G9a in the NAc and/or by differences in G9a recruitment after acute versus repeated cocaine administration.

Based on G9a's regulation of numerous plasticity-related genes in the NAc, we directly examined whether maintenance of G9a expression in this brain region after repeated cocaine treatment was sufficient to block cocaine-induced dendritic spine formation. Using a cocaine treatment protocol previously demonstrated to promote dendritic spine induction in the NAc (*20*), we examined spine density in animals injected with either HSV-GFP or HSV-G9a. In agreement with previous findings, we observed a significant increase in dendritic spine density in the NAc after cocaine treatment, an effect that was blocked completely by G9a overexpression (Fig. 3C). G9a overexpression alone was not sufficient to decrease NAc dendritic spine density in the absence of cocaine. To complement these data, $G9a^{fl/fl}$ mice received intra-NAc injections of HSV-Cre, and spine density was quantified and compared to that in animals receiving HSV-GFP in the absence of cocaine. Knockdown of G9a expression significantly increased spine density on NAc medium spiny neurons (Fig. 3C).

Given the evidence that G9a down-regulation in the NAc after repeated cocaine treatment is mediated by ΔFosB, we next examined whether this transcription factor is likewise involved in the regulation of NAc dendritic spines. Although ΔFosB has not previously been linked causally to such dendritic plasticity, several of its targets, including Cdk5 and nuclear factor–κB subunits, have been so implicated (*20*–*23*); and ΔFosB's persistent expression in NAc neurons correlates with increased dendritic spine density after repeated cocaine treatment (*27*). First, we found that induction of ΔFosB in bi-transgenic mice in the absence of cocaine, which down-regulated G9a and H3K9me2 expression (Fig. 1D, E), decreased G9a binding to numerous plasticity-related genes, many of which have also been shown to be direct targets of ΔFosB itself (Fig. 3D) (*3*, *6*). We next showed that viral overexpression of ΔFosB in the NAc significantly increased dendritic spine density under basal conditions, similar to that observed after repeated cocaine administration (Fig. 3E). Conversely, overexpression in the NAc of ΔJunD, a dominant negative mutant protein that antagonizes ΔFosB transcriptional activity, blocked the ability of repeated cocaine to increase dendritic spine formation in the NAc (Fig. 3C).

Our observation that ΔFosB regulates G9a expression in the NAc and that ΔFosB and G9a regulate some of the same target genes led us to examine other interactions between ΔFosB and G9a. After acute cocaine administration, when G9a levels were increased, binding of G9a to the *fosB* gene was increased, whereas after repeated cocaine administration, when G9a expression was suppressed, G9a binding to the *fosB* gene was decreased (Fig. 3A). Such decreased G9a binding after repeated cocaine was not observed for c-*fos,* where G9a binding is increased by repeated cocaine (fig. S7). This is consistent with the fact that, unlike *fosB*, c-*fos* is repressed, not induced, by chronic psychostimulant exposure (*5*). ΔFosB overexpression in bi-transgenic mice was sufficient to significantly decrease G9a binding to the *fosb* gene (Fig. 3D). Furthermore, G9a overexpression was sufficient to reduce increased ΔFosB expression after repeated cocaine administration (table S4). These data suggest an autoregulatory loop whereby G9a initially limits the induction of ΔFosB under acute cocaine administration. However, as ΔFosB accumulates with repeated drug exposure, it represses G9a and thereby potentiates its own further induction.

We have demonstrated that histone lysine methylation in the NAc is critically involved in regulating neuronal gene expression in response to cocaine. Repression of G9a and H3K9me2 after repeated cocaine administration promotes cocaine preference, in part through the transcriptional activation of numerous genes known to regulate aberrant forms of dendritic plasticity. Gaining a better understanding of the genes being regulated through such mechanisms will improve our knowledge of the complex biological basis of drug addiction and could aid in the development of more effective treatments for addictive disorders.

References and Notes

1. T. E. Robinson, B. Kolb, *Neuropharmacology* **47** (suppl. 1), 33 (2004).
2. S. E. Hyman, R. C. Malenka, E. J. Nestler, *Annu. Rev. Neurosci.* **29**, 565 (2006).
3. A. Kumar *et al.*, *Neuron* **48**, 303 (2005).
4. W. Renthal *et al.*, *Neuron* **56**, 517 (2007).
5. W. Renthal *et al.*, *J. Neurosci.* **28**, 7344 (2008).
6. W. Renthal *et al.*, *Neuron* **62**, 335 (2009).
7. A. Stipanovich *et al.*, *Nature* **453**, 879 (2008).
8. E. Borrelli, E. J. Nestler, C. D. Allis, P. Sassone-Corsi, *Neuron* **60**, 961 (2008).
9. K. Brami-Cherrier, E. Roze, J. A. Girault, S. Betuing, J. Caboche, *J. Neurochem.* **108**, 1323 (2009).
10. M. Tachibana, K. Sugimoto, T. Fukushima, Y. Shinkai, *J. Biol. Chem.* **276**, 25309 (2001).
11. E. J. Nestler, *Philos. Trans. R. Soc. London Ser. B* **363**, 3245 (2008).
12. C. A. McClung, E. J. Nestler, *Nat. Neurosci.* **6**, 1208 (2003).
13. M. B. Kelz *et al.*, *Nature* **401**, 272 (1999).
14. S. C. Sampath *et al.*, *Mol. Cell* **27**, 596 (2007).
15. S. Kubicek *et al.*, *Mol. Cell* **25**, 473 (2007).
16. Y. Chang *et al.*, *Nat. Struct. Mol. Biol.* **16**, 312 (2009).
17. T. E. Robinson, B. Kolb, *J. Neurosci.* **17**, 8491 (1997).
18. M. A. Ungless, J. L. Whistler, R. C. Malenka, A. Bonci, *Nature* **411**, 583 (2001).
19. M. J. Thomas, R. C. Malenka, *Philos. Trans. R. Soc. London Ser. B* **358**, 815 (2003).
20. S. J. Russo *et al.*, *J. Neurosci.* **29**, 3529 (2009).
21. J. A. Bibb *et al.*, *Nature* **410**, 376 (2001).
22. S. D. Norrholm *et al.*, *Neuroscience* **116**, 19 (2003).
23. S. Pulipparacharuvil *et al.*, *Neuron* **59**, 621 (2008).
24. H. Ujike, M. Takaki, M. Kodama, S. Kuroda, *Ann. N.Y. Acad. Sci.* **965**, 55 (2002).
25. S. Toda, H. W. Shen, J. Peters, S. Cagle, P. W. Kalivas, *J. Neurosci.* **26**, 1579 (2006).
26. D. L. Graham *et al.*, *Nat. Neurosci.* **10**, 1029 (2007).
27. K. W. Lee *et al.*, *Proc. Natl. Acad. Sci. U.S.A.* **103**, 3399 (2006).

28. This work was supported by grants from the National Institute on Drug Abuse: P01 DA08227 and R01 DA07359 (E.J.N.) and P0110044 (P.G.). E.J.N. certifies that none of the materials included in the manuscript have been previously published or are under consideration elsewhere, including on the Internet. All work involving the use of animals was conducted in accordance with institutional and Institutional Animal Care and Use Committee guidelines at both the University of Texas Southwestern Medical Center and Mount Sinai School of Medicine.

Supporting Online Material

www.sciencemag.org/cgi/content/full/327/5962/213/DC1
Materials and Methods
Fig. S1 to S8
Tables S1 to S5
References

21 July 2009; accepted 27 October 2009
10.1126/science.1179438

Supporting Online Material for

Essential Role of the Histone Methyltransferase G9a in Cocaine-Induced Plasticity

Ian Maze, Herbert E. Covington III, David M. Dietz, Quincey LaPlant, William Renthal, Scott J. Russo, Max Mechanic, Ezekiell Mouzon, Rachael L. Neve, Stephen J. Haggarty, Yanhua Ren, Srihari C. Sampath, Yasmin L. Hurd, Paul Greengard, Alexander Tarakhovsky, Anne Schaefer, Eric J. Nestler*

*To whom correspondence should be addressed. E-mail: eric.nestler@mssm.edu

Published 8 January 2010, *Science* **327**, 213 (2010)
DOI: 10.1126/science.1179438

This PDF file includes:

Essential Role of the Histone Methyltransferase G9a in Cocaine-induced Plasticity
by Maze et al.

Materials and Methods

Animals and treatments

Unless otherwise stated, mice were housed four to five per cage in a colony with a 12 hour light/dark cycle (lights on from 7:00 A.M. to 7:00 P.M.) at constant temperature (23ºC) with *ad libitum* access to water and food. All animal protocols were approved by IACUC at both UT Southwestern Medical Center and Mount Sinai School of Medicine.

For cocaine experiments [immunohistochemitry, western blotting, quantitative PCR (qPCR), microarray analysis and chromatin immunoprecipitation (ChIP)], 8- to 10-week-old male C57BL/6J mice were used. Animals received daily injections of either 'saline' (7 treatments saline, i.p.), 'acute' cocaine (6 treatments saline + one treatment 20 mg/kg cocaine-HCl, i.p.) or 'repeated' cocaine (7 treatments 20 mg/kg cocaine-HCl, i.p.). Mice were sacrificed at either 1 hour or 24 hours following the final treatment. For microarray studies, animals were treated daily with either 'saline' (15 treatments saline, i.p.), 'acute' cocaine (14 treatments saline + 1 treatment 20 mg/kg cocaine-HCl, i.p.), 'repeated + acute' cocaine (7 treatments saline + 8 treatments 20 mg/kg cocaine-HCl, i.p.) or 'repeated withdrawal + acute' cocaine (7 treatments 20 mg/kg cocaine-HCl + 7 treatments saline + 1 challenge treatment 20 mg/kg cocaine-HCl, i.p.) and were sacrificed 1 hour after the final treatment. In behavioral experiments, mice were singly housed post-surgery and were treated with 10 mg/kg cocaine-HCl, i.p. as described below. For dendritic spine analysis and microarray validation following HSV-GFP and HSV-G9a-GFP infection, mice were treated with 'saline' (5 treatments saline, i.p.) or 'repeated cocaine' (5 treatments 20 mg/kg cocaine-HCl, i.p.) over the course of 3 days, as this injection protocol has previously been demonstrated to increase spine density on nucleus accumbens (NAc) neurons within the timeframe of Herpes simplex virus (HSV) transgene expression (Supplemental ref *S1*). Mice used for dendritic spine analysis were sacrificed 4 hours following the last treatment.

To induce local deletion of the G9a transcript restricted to NAc neurons, we used mutant mice homozygous for a floxed G9a allele, which have been described in detail elsewhere (*S2*). Cre-induced recombination produces exon 22 to 25 out-of-frame splicing leading to nonsense-mediated decay of the mutated transcript. We used G9a floxed mice that were fully backcrossed to C57BL/6J mice. Mice were sterotaxically-injected into the NAc with Adeno-associated virus (AAV) vectors (serotype 2) expressing GFP or Cre-GFP between the age of 7 and 10 weeks. Immunohistochemical analysis was used to verify the efficiency of Cre-mediated recombination (see Supplemental Fig. S5). We used AAV injected animals 21 days post-surgery because recombination in G9a floxed mice was stable and maximal at this time-point, consistent with published reports (*S3-S4*). G9a and ΔJunD overexpression experiments were similarly conducted using HSV virus vectors expressing either GFP, wildtype G9a-GFP, catalytically dead G9aH1093K-GFP or ΔJunD-GFP (see *S2* for details concerning the development of G9a constructs). HSV overexpressing mice were used 3 days post-surgery since overexpression was maximal at this time-point, as observed via immunohistochemistry. Due to the transient nature of HSV expression, and the considerably more stable nature of AAV expression,

HSV vectors were used in experiments requiring fast, short-term transgene expression, whereas AAV vectors were used in experiments requiring extended periods of transgene expression. Both vectors have been shown, in extensive prior studies, to infect only neuronal cell bodies within the injected brain area, without any infection of afferent or efferent neurons.

For behavioral experiments using the pharmacological G9a/GLP inhibitor, BIX01294 (25 ng/μl), mice were sterotaxically implanted with two subcutaneous mini-pumps, as well as bilateral guide cannulae, into the NAc. Mini-pumps were activated 12 hours prior to implantation initiating the continuous delivery (0.25 μl/hour) of either vehicle (5 hydroxypropyl ß-cyclodextrin) or drug for 14 days, during which time behavioral evaluations were performed.

For ΔFosB overexpression experiments [western blotting, qPCR, and ChIP], male bitransgenic NSE-*tTA* x tetOP-Δ*FosB* mice were used (10 week-old), whereby in the absence of the tetracycline derivative doxycycline (8 weeks off doxycycline), animals displayed robust striatal restricted constitutive expression of ΔFosB (*S5*). ΔFosB overexpression in these mice was confirmed via qPCR. To confirm findings using NSE-*tTA* x tetOP-Δ*FosB* mice, wildtype 8-week-old C57BL/6J male mice were sterotaxically-injected intra-NAc with AAV vectors expressing either GFP or ΔFosB-GFP. AAV vectors were used, in this case, to ensure maximal ΔFosB expression at 8 weeks post-surgery, allowing for a direct comparison between virally infected and bitransgenic ΔFosB overexpressing mice. Viral overexpression was confirmed using qPCR at 8 weeks post-surgery (15-gauge NAc punches were dissected under the injection site). AAV-GFP and AAV-ΔFosB-GFP overexpressing mice that were not used for qPCR were treated with saline (14 treatments saline, i.p.) or repeated cocaine (14 treatments 30 mg/kg cocaine-HCl, i.p.) beginning at 6 weeks post-surgery. 4 days following the final treatment, brains were fixed with 4% paraformaldehyde, sectioned on a vibratome and used for dendritic spine analysis.

Western blot analysis

14-gauge NAc punches were taken from 1 mm coronal sections obtained using a stainless steel mouse brain matrix and were sonicated in 1 M HEPES lysis buffer (1% SDS) containing protease and phosphatase inhibitors. 10-30 μg samples of total protein were electrophoresed on 18% SDS gels. Proteins were transferred to PVDF membranes and incubated with either anti-H3K9me2 (mouse monoclonal, 1:500), anti-β-tubulin (mouse monoclonal, 1:60,000), anti-total histone H3 (rabbit polyclonal, 1:5,000), anti-GFP (used for verification of equal viral expression in punched tissue) (rabbit polyclonal, 1:1000), anti-H3K27me3 (rabbit polyclonal, 1:500) or anti-actin antibodies (mouse monoclonal, 1:60,000) overnight at 4°C (all membranes were blocked in 5% milk or 5% bovine serum albumin). Membranes were then incubated with peroxidase-labeled secondary antibodies (1:15,000-1:60,000 depending on the primary antibody used) and bands were visualized using SuperSignal West Dura substrate. Bands were quantified with NIH Image J Software and H3K9me2 bands were normalized to either actin or β-tubulin and to total histone H3 to control for equal loading. Repeated cocaine had no effect on levels of actin (Fig. S8) or total histone 3 (Fig. S1) in the NAc. Furthermore, HSV-G9a-GFP and HSV-G9aH1093K-GFP infection had no effect on total levels of β-tubulin in the NAc (Fig. S8).

Immunohistochemistry

Mice were sedated with a lethal dose of chloral hydrate and perfused with 4% paraformaldehyde before being analyzed by single or double immunohistochemistry as previously described (*S6*). Briefly, post-fixed brains were incubated at room temperature overnight in 30% sucrose before being sectioned at 35 μm (brains used for dendritic spine analysis were sectioned on a vibratome at 100 μm sections in the absence of 30% sucrose). Free-floating NAc sections were washed with 1X PBS, blocked (3% normal donkey serum, 0.1% tritonX, 1X PBS) and later incubated with anti-GFP (chicken polyclonal, 1:8000) and/or anti-G9a (rabbit polyclonal, 1:500) antibodies in blocking solution. Sections analyzed for dendritic spines were incubated with a rabbit polyclonal anti-GFP antibody at 1:200. Following overnight incubation, NAc sections were rinsed 3 times for 10 minutes with 1X PBS, followed by incubation with Cy2 and/or Cy3 fluorescent-coupled secondary antibodies in 1X PBS blocking solution for 2 hours. Sections used for morphology studies were incubated in secondary antibody overnight at room temperature. Nuclear co-staining was achieved by incubating sections in 1X PBS containing DAPI (1:50,000) for 10 minutes. Sections were once again washed, followed by ethanol dehydration and mounting with DPX. All sections were imaged using confocal microscopy.

RNA isolation and qPCR

Bilateral 14-gauge NAc punches were homogenized in Trizol and processed according to the manufacturer's instructions. RNA was purified with RNAesy Micro columns and spectroscopy confirmed that the RNA 260/280 and 260/230 rations were >1.8. RNA was then reverse transcribed using a Bio-Rad iScript Kit. cDNA was quantified by qPCR using SYBR Green. Each reaction was run in duplicate or triplicate and analyzed following the ΔΔCt method as previously described using glyceraldehyde-3-phosphate dehydrogenase (GAPDH) as a normalization control (*S7*). See supplemental Table S5 for mRNA primer sequences.

DNA microarray analysis

Four groups (3 independent biological replicates per group) were utilized for the microarray study, totaling 12 microarrays. 1 hour following the last cocaine injection, animals were rapidly decapitated and brains were removed and placed on ice. Dissections of NAc were taken using a 15-gauge needle punch and were quickly frozen on dry ice until RNA was extracted. Bilateral punches were pooled from four animals per replicate, totaling 12 mice per group. RNA isolation, microarray processing, and data analysis were performed as previously described (*S8*). Briefly, RNA was isolated and purified as described above and was checked for quality using Agilent's Bioanalyzer. Reverse transcription, amplification, labeling and hybridization to Illumina MouseWG-6 v2.0 arrays were performed using standard procedures by UT Southwestern's microarray core. Raw data were background subtracted and quantile normalized using Beadstudio software. Normalized data were analyzed using GeneSpring software and genelists were generated using significance criteria of a 1.3 fold change cutoff coupled with a non-stringent p-value cutoff of $p < 0.05$.

We maintain a high degree of confidence in these data for several reasons. First, all animals were handled, treated and killed at the same time, under the same conditions. As well, all RNA and array processing was performed at the same time. Second, we performed triplicate arrays and pooled multiple animals per array sample, thereby

minimizing differences due to individual variability and increasing statistical power (*S9*). Third, the data analysis criteria used for our study are recommended by the MicroArray Quality Control project, as these criteria have been validated to provide a high degree of intersite reproducibility and inter- and intraplatform reproducibility (*S10*-*S11*).

Construction of viral vectors

Due to viral vector insertion size constraints, coding sequences for either wildtype G9a (G9a) or catalytically dead G9a (G9aH1093K) were subcloned into the bicistronic p1005+ HSV plasmid expressing GFP under the control of the human immediate early cytomegalovirus promoter (CMV) (the G9a insertion size was ~ 3.96 kb, which exceeds the maximum insertion size for AAV-2 vectors). The IE4/5 promoter drives G9a expression. Fragments were subcloned into the bicistronic p1005+ HSV plasmid via blunt end ligations with Klenow treated PmeI and EcoRI digested G9a (from pcDNA3.1) and CIP treated p1005+ following EcoRI digestion. For production of HSV-ΔJunD-GFP, the coding sequence of ΔJunD flanked by EcoRI restriction sites was generated by PCR using primer oligonucleotides containing the EcoRI site. The PCR product was then ligated into the EcoRI site of the p1005+ vector. Local expression of Cre recombinase in NAc neurons was achieved by viral-mediated gene delivery using an AAV vector as described (*S12*). GFP or an N-terminal fusion of GFP to Cre was subcloned into a recombinant AAV-2 vector containing a CMV promoter with a splice donor acceptor sequence and polyadenylation signal. All vector insertions were confirmed by dideoxy-sequencing. Viral vectors were produced using a triple-transfection, helper-free method, as previously described (*S13*). Purified virus was stored at -80°C. Viral quality was assessed by infectious titer evaluated in HEK293 cells. AAV-ΔFosB-GFP viruses were similarly prepared. For HSV-Cre, Cre expression was driven by an IRES promoter, as opposed to the IE4/5 promoter, in order to minimize Cre expression and prevent neuronal toxicity (see *S14* for viral construction). In all cases, viral overexpression was validated, both *in vitro* and *in vivo,* via qPCR, and viruses were immunohistochemically confirmed to display NAc-restricted expression following surgery.

Stereotaxic surgery

Under ketamine (100 mg/kg)/xylazine (10 mg/kg) anesthesia, mice were positioned in a small-animal stereotaxic instrument, and the cranial surface was exposed. Thirty-three gauge syringe needles were used to bilaterally infuse 0.5 μl of virus into the NAc at a 10° angle (AP + 1.6; ML + 1.5; DV – 4.4) at a rate of 0.1 μl/min. Animals receiving HSV injections were allowed to recover for 2 days following surgery, while mice used for behavioral testing receiving AAV vectors were allowed to recover for 20 days before being subjected to place conditioning. These times are consistent with the periods of maximal viral-mediated transgene expression for the two vectors. For BIX01294 infusions, each of two mini-pumps were positioned subcutaneously on the mouse's back. Cannulae placements were achieved by drilling two small cranial holes above the NAc, and by the delivery of the cannula from bregma (AP + 1.5; ML + 1.0; DV – 5.4). Mice were allowed to recover from surgery for 4 to 5 days before beginning the place conditioning procedure to cocaine as described below.

Conditioned place preference

The place conditioning procedure was conducted as previously described, with the following modifications (*S7*). Briefly, 3 days after intra-NAc infusions of HSV-G9a-GFP, HSV-G9aH1093K-GFP or HSV-GFP, mice were placed into the conditioning

chambers, which consist of three distinct environments. Mice that showed significant preference for either of the two conditioning chambers were excluded from the study (<10% of all animals). Conditioning groups were then balanced to adjust for any chamber bias that may still exist. On subsequent days, animals were injected with saline and confined to one chamber in the afternoon for 30 minutes and then injected with cocaine (10 mg/kg, i.p.) and confined for 30 minutes to the other chamber in the evening for 2 days (two saline and two cocaine pairings). On the day of the test, mice were placed back into the apparatus without treatment for 20 minutes and tested to evaluate which side they preferred. Locomotor responses to cocaine were assessed via beam breaks in the cocaine-paired chambers to ensure effectiveness of drug treatment. For AAV and BIX01294 CPP experiments, a slightly modified protocol was employed. Animals were again injected with either saline or cocaine (10 mg/kg, i.p.) and confined to specific chambers for 30 minute sessions, but instead were only conditioned once a day for 4 days, followed by the test on day 5 (animals were conditioned in the evening and conditioning treatments were alternated). For all groups, baseline locomotion in response to saline was assessed to ensure that locomotion was not affected by viral or inhibitor treatment.

Intravenous cocaine self-administration

Male adolescent Long-Evans rats, weighing 230-250 g at the beginning of the experiment, were obtained. They were housed in a humidity- and temperature-controlled environment on a reversed 12 hour light/dark cycle (lights off at 9:00 a.m.) with *ad libitum* access to food and water. Rats were allowed to acclimate in their new environment and were handled daily for 1 week before the start of the experiment. All procedures were conducted in accordance with the National Institute of Health's Guide for the Care and Use of Laboratory Animals and were approved by Mount Sinai's Animal Care and Use Committee. The self-administration equipment was fitted with infrared beams to measure locomotor behavior. Self-administration was carried out as previously described (*S15-S16*) with catheters implanted into the right jugular vein under isoflurane (2.4-2.7%) anesthesia. Catheters were flushed with 0.1 ml of a saline solution containing 10 U heparin and ampicillin (50 mg/kg). Following one week of recovery from surgery, self-administration training began during the dark phase of the light/dark cycle. Animals were allowed 3-hour daily access to cocaine (0.75 mg/kg/infusion) under a fixed ratio-1 (FR1) reinforcement schedule, where 1 active lever press resulted in a single infusion of drug. Rats stabilized their cocaine intake after 6 days (<15% variation in response rate over 3 consecutive days, with at least 75% responding on the reinforced lever). 24 hours after the final self-administration session, rats were quickly decapitated, brains rapidly removed and processed for RNA isolation and qPCR.

Chromatin immunoprecipitation (ChIP)

Fresh NAc punches were formaldehyde cross-linked and prepared for ChIP as previously described (*S17-S18*) with minor modifications. Briefly, 4 14-gauge NAc punches per animal (5 animals pooled per sample) were collected, cross-linked with 1% formaldehyde and quenched with 2 M glycine before freezing at -80°C. 1 day prior to sample sonication, sheep anti-rabbit/mouse (depending on precipitation antibody) IgG magnetic beads were prepared by incubating appropriate magnetic beads with either anti-G9a (rabbit polyclonal ChIP grade) or anti-H3K9me2 (mouse monoclonal ChIP grade) antibodies overnight at 4°C under constant rotation in block solution. Tissue sonication

and chromatin shearing were carried out as previously described (*S17*). Following sonication, equal concentrations of chromatin were transferred to new tubes and ~5% of the final products were saved to serve as 'input' controls. After thorough washing and resuspension of the conjugated bead/antibody mixtures, equal volumes of antibody/bead mixtures (~7.5 μg antibody/sample) were added to each chromatin sample and incubated for ~16 hours under constant rotation at 4°C. Samples were further washed and reverse cross-linked at 65°C overnight before DNA purification using a PCR purification kit. Following DNA purification, samples were subjected to qPCR and were normalized to their appropriate 'input' controls as previously described (*S17*). Normal mouse IgG immunoprecipitations using a mouse polyclonal anti-IgG antibody were also carried out to control for appropriate enrichment of signal amplification. Adenine phosphoribosyltransferase (APRT) was used as a negative control for cocaine and ΔFosB overexpression experiments. See Supplemental Table S5 for promoter primer sequences.

Dendritic spine analysis

To study the role of G9a in the regulation of neuronal morphology in vivo, we used methods previously described with the following modifications (*S1*). Three days after injection of HSV-GFP, HSV-G9a-GFP, HSV-ΔJunD-GFP (all viruses were used in wildtype C57Bl/6J mice), or HSV-Cre-GFP (used in $G9a^{fl/fl}$ mice), when viral expression was maximal, mice were perfused, brains were cryoprotected and later sectioned at 100 μm on a vibratome. Sections were then immunostained using an antibody against GFP as described above (see Immunohistochemistry). To assess the effects of G9a overexpression and knockout on spine numbers, as well as the effect of ΔJunD overexpression, we measured the number of spines on approximately 1-2 neurites per neuron equaling at least 299 μm of secondary dendrites from GFP-expressing NAc medium spiny neurons (MSNs). Given that MSNs are morphologically distinct from other neuronal populations in the NAc, as well as previous reports indicating that HSV primarily infects DARPP-32 expressing neurons in this brain region (*S19*), we are confident that MSNs were exclusively assessed in these studies. For each animal, we examined ~6-8 neurons in 3-4 animals per group (7 groups), after which an average value was obtained for each animal for statistical analysis. Experiments designed to examine the effects of ΔFosB overexpression on NAc spine density were carried similarly to that described above, with the exception that AAV vectors were used to express GFP or ΔFosB-GFP for extended periods of time (8 weeks). All HSV images were captured using a confocal microscope with a 100X oil-immersion objective (AAV images were captured with a 63X oil-immersion objective). Images were acquired with the pinhole set at 1 arbitrary unit and a 1024 x 1024 frame size. Dendritic length was measured using NIH Image J software, and spine numbers were counted blind by the primary experimenter, as slides were coded prior to experimental scanning. The average number of spines per 10 μm of dendrite was calculated.

Statistical analysis

One- and two-way ANOVAs were performed to determine significance for conditioned place preference and dendritic spine analysis with greater than two groups. Student's t tests were used for other comparisons including qPCR, western blotting, dendritic spine analysis comparing HSV-GFP to HSV-Cre in $G9a^{fl/fl}$ mice, microarray analyses (see above) and chromatin immunoprecipitation experiments. Planned student's t-tests were used following two-way ANOVA analysis of dendritic spine density after

ΔFosB overexpression with confirmation of significant main effects of drug treatment and virus. All values included in the figure legends represent mean ± SEM (*$p \leq 0.05$; **$p < 0.001$). Detailed statistical analyses for Figs. 1-3 in the main text are given in: Detailed Figure Legends Including Statistics.

Supporting Text: Detailed Figure Legends Including Statistics

Fig. 1. Repeated cocaine represses G9a expression in NAc through a ΔFosB-dependent mechanism. **(A)** mRNA expression of H3K9/K27 KMTs (N = 6-10/group) and KDMs (N = 6/group) in NAc 24 hr after repeated cocaine. Significance determined using student's t-tests [(G9a-t_{17} = 2.504, *p < 0.05), (GLP-t_{17} = 2.232, *p < 0.05), (SUV39H1-t_{10} = 0.8452, p > 0.05), (SUV39H2-t_{14} = 1.412, p > 0.05), (SETDB1-t_{14} = 0.5305, p > 0.05), (EZH2-t_{10} = 1.320, p > 0.05), (JMJD2A-t_{10} = 1.241, p > 0.05), (JMJD2B-t_{10} = 0.9693, p > 0.05), (JMJD2C-t_{10} = 0.2892, p > 0.05), (LSD1-t_{10} = 0.06782, p > 0.05), (JMJD3-t_{10} = 0.4332, p > 0.05), (UTX-t_{10} = 0.4727, p > 0.05)]. **(B)** H3K9me2 levels in NAc 24 hr after repeated cocaine. H3K9me2 levels are represented as normalized values to both actin and total histone H3. Significance determined using a student's t-test [t_8 = 4.417, *p < 0.05] (N = 5/group). **(C)** Analysis of gene expression after acute or repeated cocaine. Heatmaps (*) show genes upregulated in NAc 1 hr after a cocaine challenge in naïve animals (*Acute;* 94 genes), in animals treated repeatedly with cocaine (*Repeated + acute;* 277 genes) or in animals after 168 hr withdrawal from repeated cocaine (*Repeated wd + acute*; 217 genes). Associated heatmaps show how genes were affected under the other 2 conditions. Desensitized transcriptional responses following repeated cocaine are indicated (*******). See Supplemental Tables S1-S3 for comparative gene lists. **(D)** H3K9me2 levels in NAc from NSE-*tTA* x tetOP-Δ*FosB* mice on ('ΔFosB off') and off ('ΔFosB on') doxycycline 1hr after repeated cocaine. Significance determined using a student's t-test [t_8 = 2.776, *p < 0.05] (N = 5/group). **(E)** G9a mRNA expression in NAc from NSE-*tTA* x tetOP-Δ*FosB* mice on ('ΔFosB off') and off ('ΔFosB on') doxycycline (N = 8/group), and from animals infected with AAV-GFP or AAV-ΔFosB (N = 4-6/group). Significance determined using student's t tests [(NSE-*tTA* x tetOP-t_{14} = 2.332, *p < 0.05), (AAV-ΔFosB-t_8 = 2.197, *p < 0.05)]. Data are presented as mean ± SEM.

Fig. 2. G9a in NAc regulates cocaine-induced behavioral plasticity. **(A)** Representative image of HSV-mediated transgene expression in NAc. Cartoon of the coronal brain slice was taken from the mouse brain atlas. **(B)** Conditioned place preference for cocaine in animals infected with HSV-GFP (N=19), HSV-G9a (N=13), or HSV-G9aH1093K (N=10). One-way ANOVA revealed a significant effect of G9a viral overexpression on behavior [$F_{2,39}$ = 3.560, p = 0.04]. Dunnett's multiple comparison tests demonstrated a significant decrease in cocaine preference for HSV-G9a [*p < 0.05], but not for HSV-G9aH1093K [p > 0.05]. **(C)** H3K9me2 levels in NAc of animals infected with HSV-GFP, HSV-G9a, or HSV-G9aH1093K. H3K9me2 levels were normalized to β-tubulin. HSV-G9a significantly increased global H3K9me2 levels in NAc in comparison to HSV-GFP infection [t_4 = 2.246, *p < 0.05], whereas HSV-G9aH1093K infection had no effect [t_3 = 1.189, p > 0.05] (N = 3-4/group). **(D)** Conditioned place preference for cocaine in $G9a^{fl/fl}$ animals infected with AAV-GFP or AAV-Cre. Significance determined using a student's t-test [t_{17} = 1.695, *p ≤ 0.05] (N = 9-10/group). **(E)** H3K9me2 levels in NAc of $G9a^{fl/fl}$ mice infected with AAV-GFP or AAV-Cre. H3K9me2 levels were normalized to β-tubulin. Significance determined using a student's t-test [t_2 = 2.885, *p ≤ 0.05] (N = 3/group) **(F)** Conditioned place preference for cocaine in animals receiving intra-NAc vehicle or BIX01294. Significance determined using a student's t-test [t_{22} = 2.202, *p < 0.05] (N = 12/group) **(G)** H3K9me2 levels in NAc of animals receiving intra-NAc

vehicle or BIX01294. H3K9me2 levels were normalized to β-tubulin. Significance determined using a student's t-test [$t_8 = 1.962$, *$p < 0.05$] (N = 5/group). Data are presented as mean ± SEM.

Fig. 3. G9a in NAc regulates cocaine-induced dendritic spine plasticity. **(A)** Quantitative G9a ChIP in NAc from acutely- and repeatedly-treated animals, at 1 and 24 hr respectively. APRT was used as a negative control. Data are presented as the relative fold difference from saline controls (---). Significance determined using student's t-tests [Acute-(Cdk5-$t_5 = 2.006$, *$p \leq 0.05$), (p65/NFκB-$t_6 = 2.954$, *$p < 0.05$), (Arc-$t_6 = 0.2398$, $p > 0.05$), (FosB-$t_6 = 1.931$, *$p \leq 0.05$), (LIMK-$t_5 = 2.663$, *$p < 0.05$), (BDNF IV-$t_5 = 1.109$, $p > 0.05$) (APRT-$t_6 = 0.06259$, $p > 0.05$)] [Repeated-(Cdk5-$t_4 = 12.50$, *$p < 0.05$), (p65 NFκB-$t_6 = 2.370$, *$p < 0.05$), (Arc-$t_6 = 2.363$, *$p < 0.05$), (FosB-$t_4 = 3.181$, *$p < 0.05$), (LIMK-$t_4 = 2.033$, *$p \leq 0.05$), (BDNF IV-$t_5 = 2.047$, *$p < 0.05$), (APRT-$t_6 = 0.1564$, $p > 0.05$)] (4 groups-N = 3-4/group). **(B)** Quantitative H3K9me2 ChIP in NAc from repeatedly cocaine-treated animals at 24 hr. APRT was used as a negative control. Data are presented as the relative fold difference from saline controls (---). Significance determined using student's t-tests [(Cdk5-$t_8 = 2.134$, *$p < 0.05$), (p65/NFκB-$t_4 = 7.146$, *$p < 0.05$), (Arc-$t_8 = 1.900$, *$p < 0.05$), (FosB-$t_8 = 2.249$, *$p < 0.05$), (LIMK-$t_4 = 3.528$, *$p < 0.05$), (BDNF IV-$t_4 = 2.433$, *$p < 0.05$), (APRT-$t_5 = 0.5499$, $p > 0.05$)] (N = 3-5/group). **(C)** Dendritic spine analysis in animals infected with HSV-GFP, HSV-G9a or HSV-ΔJunD following repeated cocaine, and dendritic spines in $G9a^{fl/fl}$ mice following HSV-Cre infection. A significant main effect (two-way ANOVA) of drug treatment [$F_{1,16} = 10.20$, $p = 0.016$], viral overexpression [$F_{2,16} = 19.06$, $p < 0.0001$] and interaction between drug treatment and viral overexpression [$F_{2,16} = 9.491$, $p = 0.002$] was observed. Bonferroni post-hoc analysis indicated significant differences between saline and cocaine treatment in HSV-GFP infected animals [**$p < 0.001$], and between HSV-GFP and HSV-G9a/HSV-ΔJunD overexpression with repeated cocaine treatment [**$p < 0.001$] (N = 3-4/group). G9a knockdown oppositely increased dendritic spine density on NAc neurons in comparison to HSV-GFP animals under saline conditions [$t_4 = 3.353$, *$p < 0.05$] (N = 3/group). **(D)** Quantitative G9a ChIP in NAc from NSE-*tTA* x tetOP-Δ*FosB* mice on ('ΔFosB off') and off ('ΔFosB on') doxycycline. APRT was used as a negative control. Significance determined using student's t-tests [Cdk5-$t_5 = 3.034$, *$p < 0.05$), (p65/NFκB-$t_6 = 2.048$, *$p < 0.05$), (FosB-$t_6 = 2.356$, *$p < 0.05$), (APRT-$t_5 = 0.1042$, $p > 0.05$)] (N = 3-4/group). **(E)** Dendritic spine analysis in animals infected with AAV-GFP or AAV-ΔFosB following repeated cocaine. A significant main effect (two-way ANOVA) of drug treatment [$F_{1,12} = 4.603$, $p = 0.05$] and viral overexpression [$F_{1,12} = 7.902$, $p = 0.02$] was observed. Planned student's t tests indicated significant differences in AAV-GFP infected animals following cocaine treatment [$t_6 = 2.435$, *$p \leq 0.05$], between AAV-GFP and AAV-FosB infected animals under saline treatment conditions [$t_6 = 2.729$, *$p < 0.05$] and between AAV-GFP saline and AAV-Δ FosB under cocaine treatment conditions [$t_6 = 2.888$, *$p < 0.05$](N = 4/group). Data are presented as mean ± SEM.

Supporting Figures and Tables

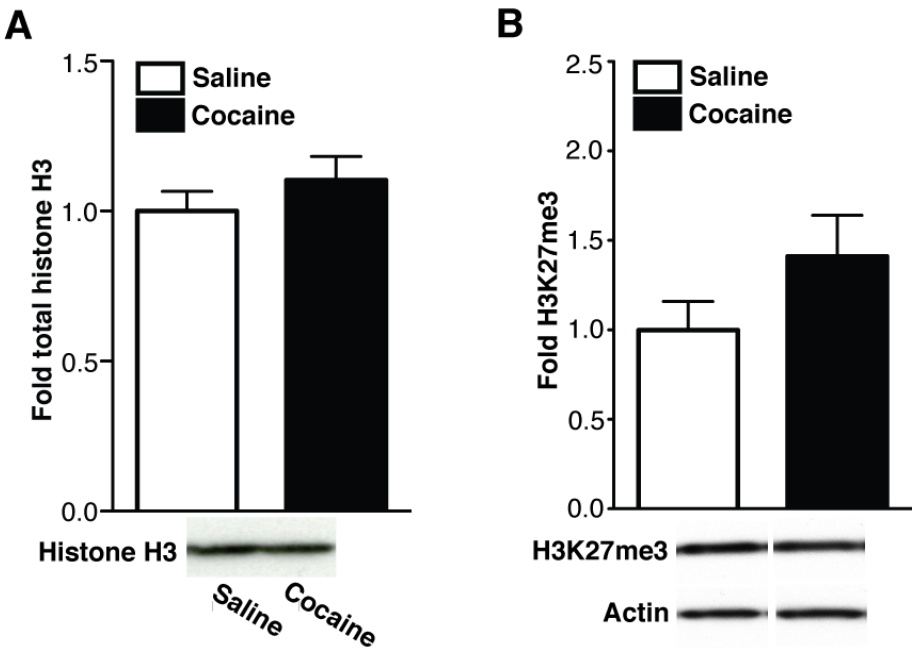

Fig. S1. Levels of total histone H3 and of H3K27me3 are unaffected in NAc by repeated cocaine. **(A)** Histone H3 and **(B)** H3K27me3 levels 24 hr following repeated cocaine. Significance determined using student's t-tests [(Total histone H3-$t_{12} = 0.9941$, $p > 0.05$), (H3K27me3-$t_{12} = 1.523$, $p > 0.05$)] (N = 6-8/group). Data are presented as mean ± SEM.

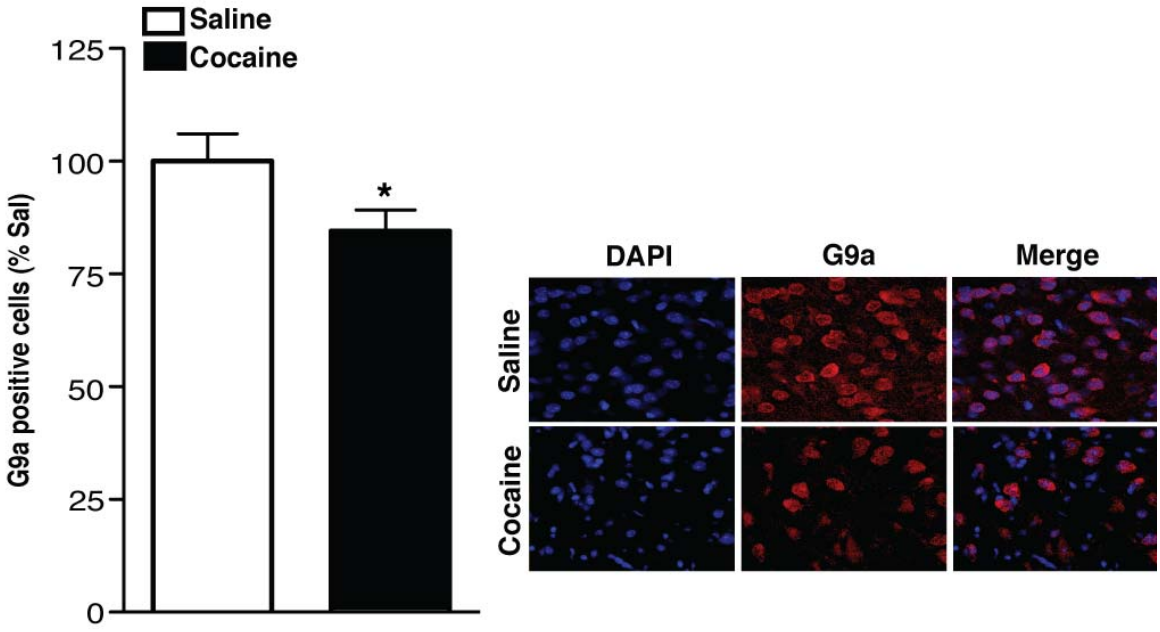

Fig. S2. G9a protein expression is decreased following repeated cocaine. G9a protein expression in NAc, measured by immunohistochemistry, 24 hr following repeated cocaine. ~119 DAPI positive cells were counted and averaged per animal (40X objective). Significance determined using a student's t test [$t_6 = 2.011$, *$p < 0.05$] (N = 3-4/group). Data are presented as mean ± SEM. Note that the specificity of G9a immunoreactivity was confirmed by showing its complete loss upon knockout of G9a (see Supplemental Fig. S5).

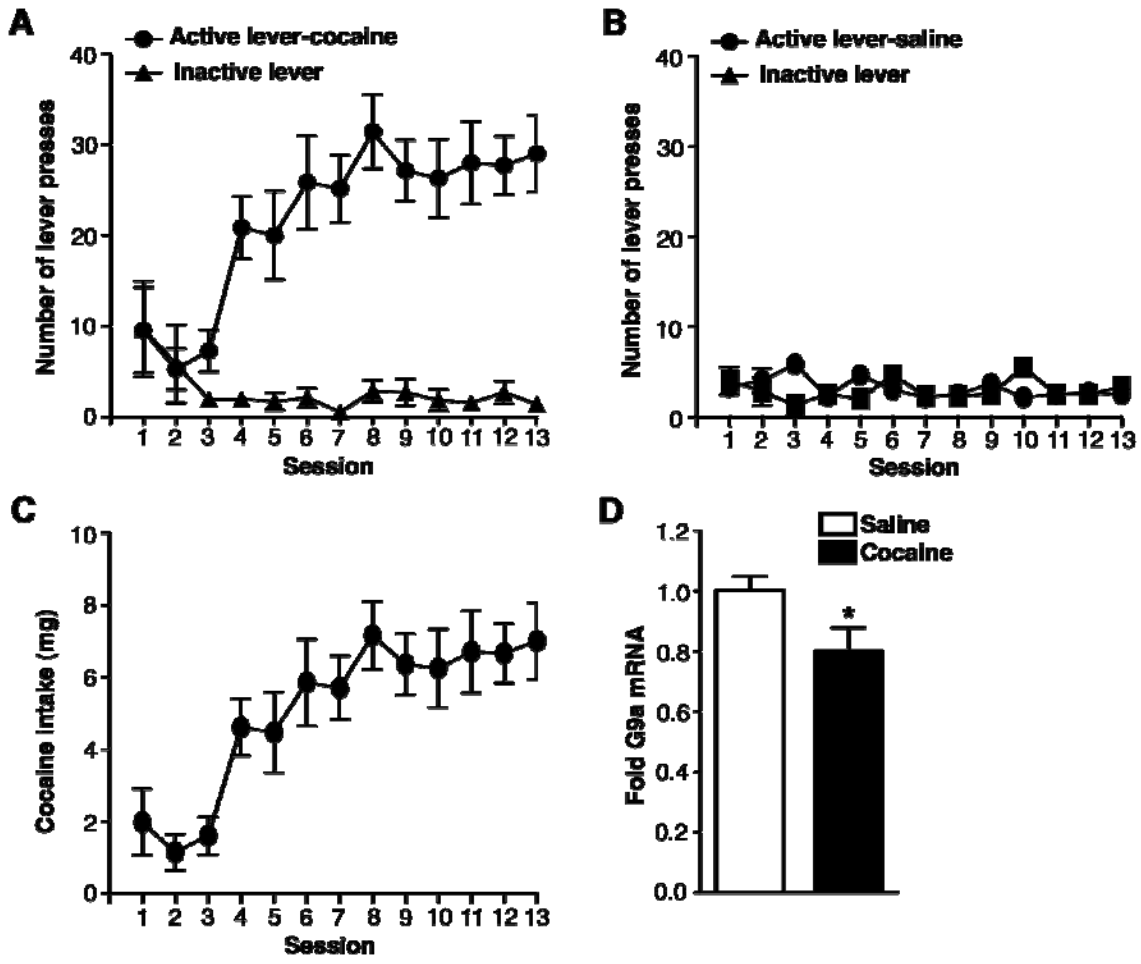

Fig. S3. Cocaine self-administration reduces G9a expression in the NAc. **(A)** The number of lever presses on the 'active' and 'inactive' levers for each daily session of cocaine self-administration, whereby 'active' lever pressing resulted in cocaine infusions (0.75 mg/kg/infusion). **(B)** 'Active' lever pressing resulted in saline infusions for control animals. Lever pressing of the 'inactive' lever in both circumstances was without consequence. **(C)** Animals trained to self-administer cocaine stabilized their cocaine intake after 6 days, with <15% variation in response rate over three consecutive days. **(D)** G9a mRNA expression 24 hr following repeated cocaine self-administration. Significance determined using a student's t test [$t_{12} = 2.170$, $^*p \leq 0.05$] (N = 7/group for all conditions). Data are presented as mean ± SEM.

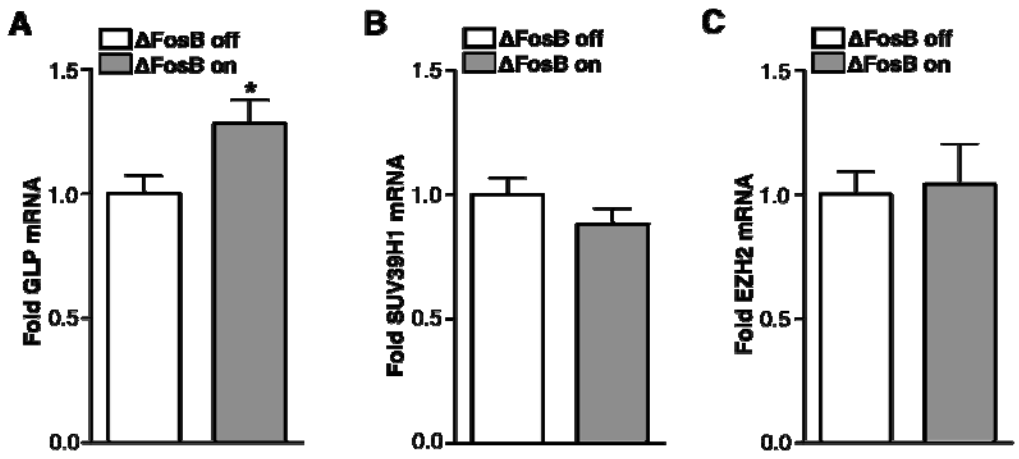

Fig. S4. ΔFosB-mediated repression of histone methylation is G9a specific. mRNA expression of **(A)** GLP, **(B)** SUV39H1 and **(C)** EZH2 in NAc from NSE-*tTA* x tetOP-Δ*FosB* on ('ΔFosB off') and off ('ΔFosB on') doxycycline. Significance determined using student's t tests [(GLP-t_{13} = 2.360, *$p < 0.05$), (SUV39H1-t_{13} = 1.256, $p > 0.05$), (EZH2-t_{13} = 0.2214, $p > 0.05$)] (N = 7-8/group). Data are presented as mean ± SEM.

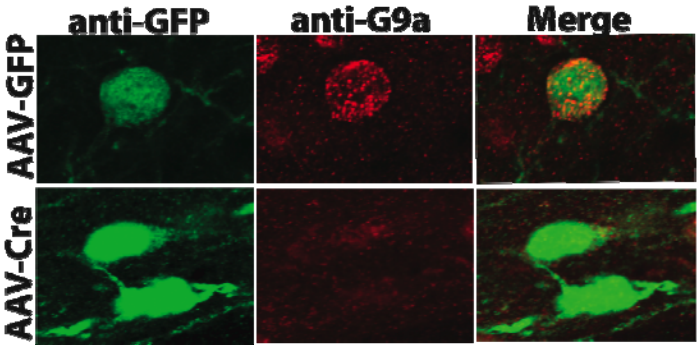

Fig. S5. AAV-Cre mediated knockdown of G9a in NAc MSNs. $G9a^{fl/fl}$ mice injected with AAV-GFP or AAV-Cre-GFP. Immunohistochemical analysis confirmed G9a knockdown in NAc neurons of $G9a^{fl/fl}$ mice infected with AAV-Cre-GFP 21 days post-surgery.

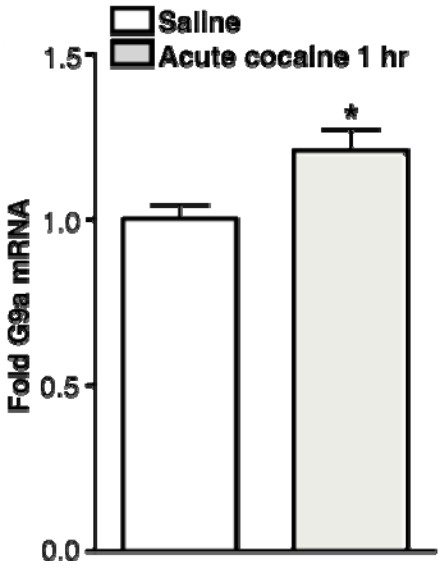

Fig. S6. Acute cocaine increases G9a expression in the NAc. G9a mRNA expression 1 hr following acute cocaine. Significance determined using a student's t test [$t_{12} = 2.442$, *$p < 0.05$] (N = 6-8/group). Data are presented as mean ± SEM.

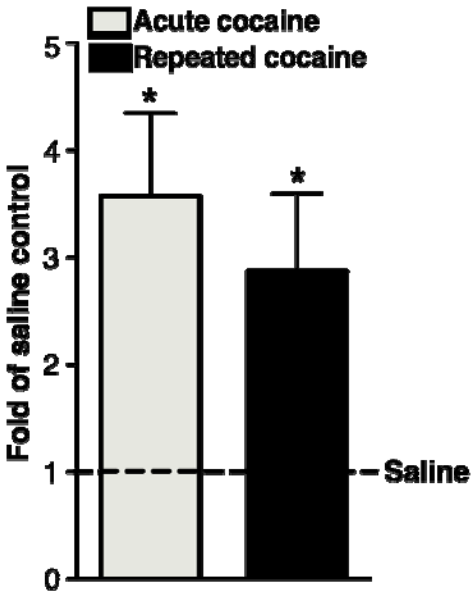

Fig. S7. G9a binding to the *c-fos* promoter is increased following both acute and repeated cocaine administration. Quantitative G9a ChIP in NAc from acutely- and repeatedly-treated animals, at 1 and 24 hr, respectively. Significance was determined using student's t-tests [(Acute cocaine 1 hr-$t_5 = 2.676$, *$p < 0.05$), (Repeated cocaine 24 hr-$t_4 = 2.578$, *$p < 0.05$)] (4 groups-N = 3-4/group (5 animals pooled/N). Data are presented as mean ± SEM.

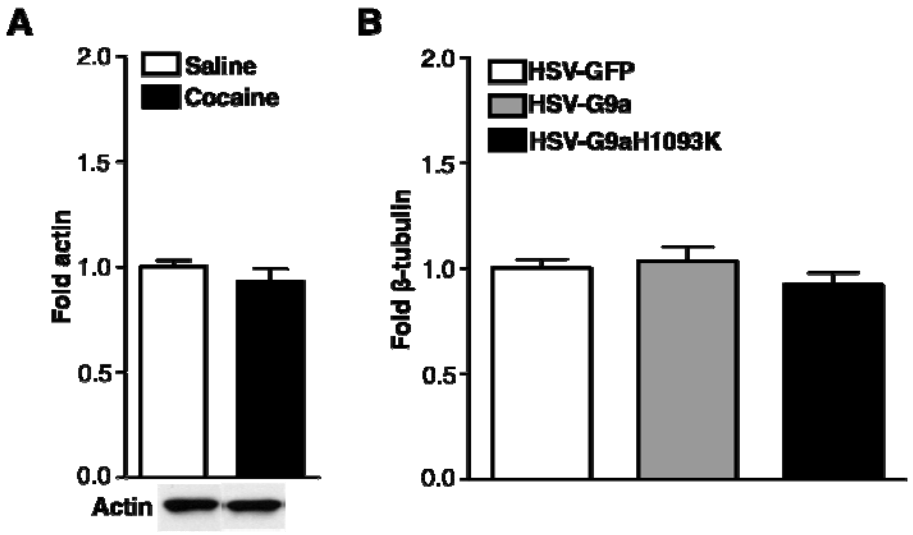

Fig. S8. Levels of actin and β-tubulin, used as loading controls on western blots, are unaffected by repeated cocaine and viral overexpression. **(A)** Actin levels 24 hr following repeated cocaine. Significance was determined using a student's t test [t_9 = 0.9399, $p > 0.05$] (N = 5-6/group). **(B)** β-tubulin 3 days following infection with HSV-GFP, HSV-G9a-GFP, or HSV-G9aH1093K-GFP [$F_{2,13} = 0.8934$, $p > 0.05$] (N = 4-8/group). Data are presented as mean ± SEM.

Table S1. Gene List: Acute (94 Genes)
***Desensitized Transcriptional Responses (<1.1 Fold Induction 'Repeated + Acute' Cocaine)

Illumina ID	Gene Symbol	Acute	Repeated + Acute	Repeated WD + Acute
5310672	FXYD5***	1.399	0.887	0.896
6770053	SH3KBP1***	1.439	0.924	1.248
1190619	MAN2B2***	1.626	0.937	0.981
3890348	9030418K01RIK***	1.389	0.946	0.894
360435	NDE1***	1.508	1.061	1.105
2810221	CDK5RAP1***	1.351	1.063	1.043
780358	BRAP***	1.419	1.078	1.092
6380376	DUSP14***	1.302	1.089	1.048
5910193	1110059P08RIK***	1.41	1.095	1.24
3400026	ASPH	2.052	1.101	1.749
4180520	GNAS	1.467	1.107	1.102
360047	ZFP312	1.354	1.112	1.166
4880253	JMJD3	1.314	1.112	0.906
150431	ADPRT2	1.429	1.117	1.224
6280376	5830457O10RIK	1.306	1.131	1.15
5550519	TAOK1	1.304	1.132	0.969
7400671	HS6ST2	1.333	1.141	1.026
4390010	CCDC39	1.339	1.152	1.092
6660427	TIMP3	1.366	1.16	1.157
6620156	4933424A20RIK	1.373	1.161	1.332
3940296	UBQLN1	1.303	1.161	1.142
6900706	GRIA3	1.302	1.166	1.236
3180026	BAALC	1.315	1.172	1.211
4260709	GSN	1.488	1.176	0.991
6560682	CHD4	1.32	1.178	1.14
5820500	PDXDC1	1.364	1.18	1.314
6620079	EGR1	1.316	1.187	1.156
2710047	JMJD2A	1.418	1.188	1.074
1710296	MLX	1.322	1.193	1.259
5260358	CHD2	1.308	1.193	0.954
670601	6430704M03RIK	1.425	1.206	1.238
1260719	KIFAP3	1.302	1.206	1.273
2360431	ABCF1	1.322	1.208	1.221
650253	PPM2C	1.32	1.214	1.014
5340470	CCDC15	1.31	1.216	1.098
4290278	FOXC1	1.353	1.236	1.272
6020300	ZFP449	1.349	1.24	1.329

20154	MIDN	1.377	1.242	1.09
1050176	MAN1A2	1.448	1.246	1.216
2750551	GPR75	1.504	1.247	1.37
2600296	CUL4A	1.333	1.249	1.055
1990612	SLC6A15	1.434	1.251	1.28
5900747	ECHDC1	1.695	1.257	1.064
1580343	TM9SF2	1.399	1.272	1.186
5550619	NCOA2	1.365	1.289	1.484
4880008	ARL6IP2	1.328	1.292	1.342
3130719	CREM	1.452	1.293	1.283
1660678	TMEM129	1.317	1.297	1.327
6510189	MTF1	1.598	1.3	1.408
3840709	ENDOGL1	1.446	1.301	1.264
10176	DUSP4	1.4	1.305	1.194
7560367	ADCY1	1.302	1.324	1.269
840102	D030038A19RIK	1.399	1.336	1.492
6940255	DUSP6	1.393	1.339	0.999
4560681	EGR4	1.612	1.342	1.129
1820035	CASP6	1.332	1.344	1.182
2810196	SCL0002012.1_0	1.317	1.351	1.211
3940044	HGS	1.57	1.37	1.132
4180592	4930429A08RIK	1.402	1.377	1.269
3520630	TGOLN1	1.325	1.386	1.283
4480494	4930487N19RIK	1.337	1.388	1.335
4070400	RND3	1.501	1.39	1.249
1070450	RLBP1L1	1.505	1.396	1.412
3370719	IDS	1.445	1.396	1.183
7000241	RTN3	1.327	1.396	1.431
5570041	HOMER1	1.316	1.397	1.12
6560195	CLK4	1.356	1.407	1.36
1690019	MEST	1.538	1.422	1.257
2630068	CCDC77	1.378	1.429	1.443
7400044	FOSL2	1.644	1.441	1.289
3120014	JUNB	1.596	1.441	1.233
5270195	P4HA1	1.317	1.457	1.316
1410368	HIST1H4D	1.621	1.471	1.506
1430315	5830435K17RIK	2.055	1.472	1.462
2570543	MAGI3	1.607	1.477	1.228
2680093	NCOA6	1.748	1.479	1.399
1470386	ASAH3L	1.348	1.483	1.436
7550523	LMBR1	1.576	1.487	1.538
3400072	9830165L15RIK	1.364	1.511	1.469
1030398	2610207F23RIK	1.688	1.534	1.338

2940598	A830005C06RIK	1.576	1.538	1.366
5860736	B230339M05RIK	1.598	1.545	1.398
7160132	A630082K20RIK	1.37	1.57	1.446
2360343	C330006P03RIK	1.598	1.574	1.414
290553	D930015A08RIK	1.7	1.614	2.059
5050768	CUGBP1	1.379	1.675	1.537
1450095	ICAM1	1.452	1.723	2.079
2510564	GCA	1.918	1.728	2.047
1780239	4632408O18RIK	1.708	1.733	1.374
5860433	OSP94	1.376	1.78	1.582
2100470	IL1RAP	1.469	1.872	1.993
7330026	EGR2	2.977	2.121	1.389
5560639	CNTN4	2.113	2.237	2.443
1050598	MON1A	2.235	2.274	2.012

Table S2. Gene List: Repeated + Acute (277 Genes)

Illumina ID	Gene Symbol	Acute	Repeated + Acute	Repeated WD + Acute
2350017	HSPA1A	1.807	4.256	3.056
6620142	PCDHB17	1.383	2.434	1.635
510368	FOS	2.165	2.367	2.212
7330026	EGR2	2.701	2.338	1.389
4070066	LOC381539	1.36	1.985	1.527
3460669	SPAG9	1.588	1.958	1.55
7200373	FBXO45	0.92	1.899	1.166
3400523	NPAS4	1.667	1.886	1.583
1740048	USP9X	1.962	1.874	2.205
2450048	CYLN2	1.246	1.849	1.288
3450035	HSPA1B	1.985	1.815	1.654
780592	LOC227995	1.339	1.77	1.714
6280110	D230021E06RIK	1.135	1.765	1.779
2970674	E130307A14RIK	1.137	1.76	1.47
6580373	LOC280487	1.255	1.75	1.551
1780239	4632408O18RIK	1.701	1.741	1.374
2510564	GCA	1.909	1.736	2.047
4390747	A630064P09RIK	1.33	1.723	1.399
10044	GNAQ	1.343	1.714	1.174
5860433	OSP94	1.438	1.703	1.582
240707	1110062G22RIK	1.375	1.694	1.624
2100470	IL1RAP	1.634	1.683	1.993
4810112	RAB3C	0.989	1.68	1.26
3940435	MXRA8	1.679	1.664	1.246
2760519	LOC329575	0.933	1.656	1.541
6420520	FOSB	1.549	1.656	1.333
5550685	RAB14	1.151	1.652	1.704
60747	D230019G01RIK	1.204	1.647	1.532
1030398	2610207F23RIK	1.595	1.625	1.338
1990162	A830048E23RIK	1.178	1.619	1.329
1450095	ICAM1	1.545	1.618	2.079
5050768	CUGBP1	1.428	1.617	1.537
1980577	PRKWNK3	0.962	1.615	1.428
4230484	6430573H23RIK	1.283	1.615	1.543
5340132	ZZZ3	1.077	1.613	1.562
5960367	BC068281	1.152	1.609	1.33
6180471	6330532E14RIK	1.169	1.608	1.556
7160162	PSME4	1.296	1.605	1.396

3290379	BC053749	1.495	1.598	1.115
6200053	EIF2C3	1.255	1.595	1.373
290553	D930015A08RIK	1.722	1.593	2.059
770152	GRM7	1.235	1.589	1.606
5900523	TGS1	0.708	1.584	0.939
4610458	FTSJ2	1.331	1.584	1.283
1090241	MYOHD1	1.223	1.574	1.286
10008	TNKS	1.301	1.573	1.345
870561	IL1RAPL1	0.961	1.573	1.584
2810167	TGFBR1	0.786	1.568	1.215
430706	LOC672274	0.835	1.568	1.014
1690082	LOC670356	1.222	1.567	1.544
6770356	MEST	1.26	1.563	1.343
2680348	SLC35A3	1.388	1.563	1.507
6250608	BIRC6	1.381	1.561	1.413
3400072	9830165L15RIK	1.321	1.56	1.469
6370520	TNFRSF25	1.123	1.557	1.199
7650754	LOC639396	0.976	1.557	1.253
1780451	LOC100040085	1.126	1.556	1.259
5860736	B230339M05RIK	1.601	1.542	1.398
6420519	B130038B15RIK	1.344	1.54	1.492
1690019	MEST	1.423	1.538	1.257
1430035	RALGPS1	1.35	1.536	1.232
2650243	1700015F03RIK	1.254	1.534	1.149
2940598	A830005C06RIK	1.581	1.534	1.366
3460021	ABCF3	1.1	1.534	1.63
1450541	FRMPD1	1.482	1.529	1.234
3120630	PTBP2	1.4	1.528	1.298
1410368	HIST1H4D	1.561	1.527	1.506
610079	B930008G09RIK	1.118	1.525	1.595
2510324	TRPC1	1.323	1.523	1.426
3930093	LOC100043821	1.333	1.514	1.292
2510243	DDHD2	1.107	1.514	1.403
50347	9430034D17RIK	1.143	1.513	1.188
4200014	D130086K05RIK	1.02	1.513	1.589
10209	TMEM161B	1.122	1.508	1.236
3610072	BICD1	1.36	1.507	1.449
7160132	A630082K20RIK	1.43	1.504	1.446
2370575	ROCK2	1.384	1.501	1.468
4850102	A430103B12RIK	1.072	1.501	1.298
1470386	ASAH3L	1.334	1.499	1.436
2360343	C330006P03RIK	1.68	1.497	1.414
870255	SLC9A6	1.253	1.493	1.091

520129	5730433N10RIK	0.995	1.492	1.368
6980687	1110054O05RIK	1.001	1.485	1.111
7400044	FOSL2	1.604	1.477	1.289
5670424	PER2	1.179	1.476	1.195
2030093	RIPK5	1.112	1.475	1.186
1850554	ESD	0.955	1.474	0.83
520286	PHXR4	1.073	1.467	1.313
4200021	B930029N08RIK	1.041	1.462	1.432
5270195	P4HA1	1.313	1.462	1.316
4810307	ZFYVE16	1.087	1.461	1.444
6560195	CLK4	1.307	1.46	1.36
5900497	PER2	1.087	1.459	1.167
7560358	SEC22L3	1.029	1.459	1.252
6370500	DYNC2H1	1.18	1.458	1.267
610372	6430402H23RIK	1.094	1.457	1.404
4010349	6720477C19RIK	1.176	1.457	1.625
4560681	EGR4	1.486	1.456	1.129
5260176	NEO1	1.08	1.452	1.34
1300020	VPS26A	1.286	1.449	1.345
870520	2900006K08RIK	1.183	1.448	1.236
4540020	DNAJB1	1.187	1.447	1.335
4010239	ATP7A	1.119	1.446	1.552
7330360	ITGAV	1.177	1.443	1.41
7210088	NPAT	0.815	1.441	1.062
2680093	NCOA6	1.795	1.44	1.399
1430315	5830435K17RIK	2.101	1.44	1.462
7160315	B930097H17RIK	1.234	1.435	1.734
5670279	GLI2	1.131	1.435	1.217
3440692	SPRY4	1.042	1.433	1.372
3420437	9030612E09RIK	1.306	1.432	1.128
3840576	B430007K19RIK	1.08	1.43	1.303
670136	A930002F06RIK	1.259	1.429	1.542
7400121	RAB3C	1.033	1.429	1.089
3440600	LOC100047226	1.195	1.429	1.285
6650097	MIS12	0.884	1.427	1.098
1400047	4932415A06RIK	0.993	1.427	1.544
1710181	CELSR1	1.163	1.427	1.164
160402	OGN	1.244	1.425	1.266
3870739	5930407M05RIK	1.292	1.424	1.102
2260382	HEPH	1.058	1.416	1.115
460102	NUP50	1.064	1.415	1.296
1660093	BTAF1	1.147	1.414	1.273
2140398	ABCA8B	1.21	1.414	1.279

5570424	ZFP248	1.268	1.412	1.669
3520630	TGOLN1	1.303	1.41	1.283
1580561	C230091E20RIK	0.986	1.41	1.349
2360520	TBC1D1	1.281	1.41	1.354
6520484	EIF4G2	1.26	1.408	1.349
1820035	CASP6	1.272	1.407	1.182
6280605	ATM	0.999	1.407	1.096
3830136	CCNG1	1.108	1.407	1.288
2340070	4732423E21RIK	1.156	1.406	1.374
3310446	C630030A18RIK	1.088	1.406	1.485
3370719	IDS	1.435	1.406	1.183
7320041	PCDHGB6	1.042	1.405	1.25
7550523	LMBR1	1.673	1.401	1.538
4050292	B3GALNT2	1.183	1.4	1.455
7210255	ZFP654	1.126	1.399	1.307
2940500	RAI1	1.022	1.396	1.441
2100243	KIF1B	1.21	1.394	1.37
4480494	4930487N19RIK	1.331	1.394	1.335
610039	E130016E03RIK	1.231	1.39	1.228
1400035	LOC100045628	1.124	1.389	1.079
4200100	DUSP1	1.295	1.389	1.26
2480343	A430106G13RIK	1.264	1.388	1.387
6560477	SLK	1.219	1.387	1.255
2630068	CCDC77	1.425	1.382	1.443
4010064	C030045D06RIK	0.864	1.382	1.273
5670543	FBXO3	1.114	1.382	1.073
4070400	RND3	1.511	1.381	1.249
6510100	E330027P06RIK	1.171	1.381	1.363
460528	2010015J01RIK	1.123	1.381	1.025
6840500	A530010L13RIK	1.27	1.381	1.638
3400014	SLK	1.119	1.38	1.42
7000241	RTN3	1.344	1.379	1.431
7040343	OSBPL8	1.112	1.378	1.368
150543	TMEM82	0.991	1.377	1.038
1090719	CXXC5	1.105	1.377	1.058
2480224	B230337C21RIK	1.14	1.376	1.38
3420709	9330177P18RIK	1.368	1.376	1.174
4610424	TBC1D12	0.864	1.375	1.028
4730435	D030040K20RIK	1.231	1.375	1.432
6940093	6330444G18RIK	1.061	1.374	1.366
1710075	C130060B01RIK	1.116	1.374	1.221
1780242	D130057F13RIK	1.006	1.373	1.37
5220465	KCNMA1	1.126	1.372	1.395

840224	2610301N02RIK	1.198	1.371	1.161
4060017	CDC73	1.145	1.37	1.274
840451	ANKRD45	1.157	1.368	1.096
5820086	CACNB2	1.079	1.368	1.196
4850292	9530065M15RIK	0.714	1.368	1.367
150398	HECW2	1.285	1.366	1.364
1780324	CCR5	1.124	1.366	1.415
290504	SLC22A4	0.897	1.366	1.096
2970292	GABRG3	1.247	1.366	1.309
2230097	ELMO1	0.983	1.365	1.179
3400164	JAM2	1.032	1.365	1.306
5570041	HOMER1	1.349	1.363	1.12
3840709	ENDOGL1	1.382	1.362	1.264
3170451	ZSCAN20	1.062	1.361	1.343
870328	PTPN12	1.145	1.359	1.301
1450746	A930039N10RIK	1.165	1.357	1.257
4280121	D4ERTD681E	1.189	1.357	1.359
5310411	WDR45L	0.908	1.357	1.22
4280189	PAK2	1.219	1.357	1.271
3460386	RNF14	1.221	1.356	1.174
2190040	LRRTM2	1.257	1.355	1.24
1430594	FNIP1	1.065	1.355	1.298
1340270	CCNC	1.05	1.355	1.289
1240131	XPR1	1.122	1.354	1.148
5260010	PPP2R1B	1.114	1.352	1.22
1780707	9530053J19RIK	1.079	1.351	1.234
240349	HECW1	1.163	1.351	1.323
2230202	PPNR	1.003	1.351	1.534
4050612	FBXO11	1.228	1.35	1.42
4540102	BC030499	1.044	1.35	1.185
3390470	9630013P03RIK	0.936	1.35	1.187
4290474	A930007F16RIK	0.919	1.348	1.381
1170152	CLTC	1.097	1.347	1.361
3130441	MCCC1	1.05	1.346	1.078
4850066	B230310H07RIK	1.334	1.345	1.498
830463	KLHL9	1.364	1.345	1.317
4830201	LOC432730	1.1	1.345	1.28
2900041	SLC25A36	1.218	1.344	1.33
1850341	HSPG2	1.071	1.344	1.154
3120014	JUNB	1.711	1.344	1.233
5900474	SCN3B	1.188	1.344	1.157
7000112	ZWINT	1.05	1.343	1.204
3390608	4732471D19RIK	0.929	1.342	1.412

830504	4631422C13RIK	1.08	1.342	1.207
5080132	CUGBP1	1.214	1.341	1.268
3290270	HSP105	1.188	1.339	1.153
6100465	TRPS1	1.182	1.338	1.402
3840521	LOC100046232	1.216	1.337	1.335
7050692	A830006J06RIK	0.87	1.337	1.3
670487	E430026H10RIK	1.263	1.335	1.45
5900692	PTPN12	1.241	1.335	1.459
4890097	9830134K01RIK	1.231	1.335	1.181
1780132	IMPACT	1.067	1.334	1.24
4070747	4933407L23RIK	1.083	1.334	1.292
7320300	LOC381443	1.145	1.334	1.398
4540270	PKP4	1.046	1.333	1.016
3370333	GALC	1.134	1.332	1.281
6280608	DNM1L	1.072	1.332	1.195
1300739	4632413C10RIK	1.149	1.332	1.259
1090669	APRIN	1.223	1.332	1.38
5420050	0610007P08RIK	0.981	1.332	1.285
6480328	C130048M12RIK	1.057	1.332	1.398
1580343	TM9SF2	1.336	1.331	1.186
4760402	TBL1X	1.16	1.33	1.296
6290441	LOC280487	1.385	1.33	1.377
4760292	NETO2	1.183	1.329	1.326
7380162	NPHP1	1.134	1.329	1.052
2850259	SYNE1	1.261	1.328	1.39
1230021	4932410M19RIK	0.912	1.327	1.114
2070390	B230353O14RIK	1.066	1.327	1.492
1110538	PREI4	1.067	1.326	1.224
2750398	IPMK	1.246	1.326	1.349
5220112	A530024C08RIK	1.243	1.326	1.353
5360253	B830007D08RIK	1.158	1.325	1.201
7650470	0610010F05RIK	1.19	1.323	1.274
2490092	AP2B1	1.064	1.321	1.29
7100519	CLK4	1.165	1.32	1.214
2710494	F630038O13RIK	1.313	1.32	1.419
3840451	SOS2	0.988	1.319	1.156
650189	3632431M01RIK	1.089	1.318	1.288
1440286	HECTD2	1.102	1.318	1.218
3440717	RORB	1.076	1.318	1.48
50520	DGKB	1.279	1.315	1.29
6100646	PHF6	1.125	1.315	1.131
6290386	C130023A14RIK	1.088	1.314	1.198
4200017	CISH	1.189	1.313	1.101

7510315	TRIM33	1.192	1.313	1.327
7330324	MSL2L1	1.296	1.313	1.446
3440465	RABEP1	1.058	1.313	1.342
6330274	A130047F11RIK	1.226	1.312	1.32
4390142	A130084P08RIK	0.999	1.312	1.169
4070497	1700013G10RIK	1.079	1.312	1.245
6760736	EML5	1.191	1.311	1.405
520168	PHKA1	0.958	1.311	1.096
5490609	CCT7	1.211	1.309	1.121
3170072	TRIP12	0.995	1.307	1.144
2630010	MDGA2	0.955	1.306	1.157
4780446	CCDC117	1.226	1.306	1.2
4610669	ARHGAP18	0.906	1.306	1.316
3610093	PCDH9	1.082	1.306	1.23
6450037	LOC381940	1.159	1.306	1.244
3780278	A030001L21RIK	1.037	1.304	1.313
20025	PCGF6	1.179	1.303	1.305
4250373	SORBS1	1.051	1.303	1.098
1070632	SPAG9	1.064	1.303	1.364
5090551	4833438J18RIK	1.111	1.302	1.491
20066	SLC38A2	1.063	1.302	1.268
5870440	CSPG5	1.271	1.301	1.33
2940487	PPM2C	1.218	1.3	1.32
6510348	SGPL1	0.864	1.3	0.968

Table S3. Gene List: Repeated WD + Acute (217 Genes)

Illumina ID	Gene Symbol	Acute	Repeated + Acute	Repeated WD + Acute
2350017	HSPA1A	1.807	4.356	2.985
5560639	CNTN4	2.469	2.237	2.091
2510564	GCA	1.909	1.728	2.057
290553	D930015A08RIK	1.722	1.614	2.033
1450095	ICAM1	1.545	1.723	1.953
6280110	D230021E06RIK	1.135	1.624	1.934
6620142	PCDHB17	1.383	2.098	1.897
7160315	B930097H17RIK	1.234	1.329	1.873
3400026	ASPH	1.932	1.101	1.858
2100470	IL1RAP	1.634	1.872	1.791
4070066	LOC381539	1.36	1.718	1.764
1050598	MON1A	2.597	2.274	1.732
5570358	BCL2	1.588	1.48	1.715
4570450	D230010O12RIK	1.185	1.374	1.71
3460669	SPAG9	1.588	1.807	1.679
4900575	ZFP52	1.117	1.297	1.666
2680348	SLC35A3	1.388	1.423	1.654
610079	B930008G09RIK	1.118	1.48	1.642
2230202	PPNR	1.003	1.271	1.63
3460021	ABCF3	1.1	1.534	1.629
6330315	SCL0001602.1_506	1.073	1.262	1.622
2060270	ARL13B	1.049	1.094	1.622
1690082	LOC670356	1.222	1.498	1.615
870561	IL1RAPL1	0.961	1.549	1.608
5570424	ZFP248	1.268	1.483	1.588
3800133	NUMB	1.333	1.348	1.587
6580373	LOC280487	1.255	1.713	1.585
3610072	BICD1	1.36	1.382	1.58
60747	D230019G01RIK	1.204	1.603	1.574
1980577	PRKWNK3	0.962	1.47	1.569
4200014	D130086K05RIK	1.02	1.532	1.569
3440717	RORB	1.076	1.244	1.569
4180288	NFIB	1.078	1.302	1.568
1410368	HIST1H4D	1.561	1.471	1.564
580136	BVES	1.229	1.362	1.546
7000129	LOC627912	1.593	1.189	1.544
4390674	9430077D24RIK	1.077	1.242	1.531
4200021	B930029N08RIK	1.041	1.372	1.525
1070707	MAP3K10	1.294	1.229	1.524
3400072	9830165L15RIK	1.321	1.511	1.517

5860433	OSP94	1.438	1.78	1.513
6770356	MEST	1.26	1.388	1.512
670136	A930002F06RIK	1.259	1.463	1.507
2750189	NAMPT	1.429	1.73	1.505
6960136	C030038O19RIK	0.952	1.325	1.504
2370037	LOC100048616	1.165	1.247	1.504
840102	D030038A19RIK	1.392	1.336	1.5
3800427	EPB4.1L5	0.945	1.251	1.497
650475	TMF1	1.306	1.163	1.496
6180471	6330532E14RIK	1.169	1.674	1.495
110131	D430021F02RIK	1.057	1.278	1.493
5090551	4833438J18RIK	1.111	1.301	1.492
5340132	ZZZ3	1.077	1.69	1.491
7320300	LOC381443	1.145	1.251	1.49
6250608	BIRC6	1.381	1.482	1.488
5050768	CUGBP1	1.428	1.675	1.483
1660450	TMTC4	1.151	1.282	1.477
1170278	PCDH7	0.812	1.102	1.477
5900692	PTPN12	1.241	1.323	1.472
730544	ELAC2	1.059	1.221	1.466
7550603	SORBS2	1.147	1.278	1.464
7100259	MME	1.251	1.48	1.462
4060280	MBTPS2	1.255	1.103	1.461
6580279	B130017I01RIK	1.286	1.385	1.456
2940500	RAI1	1.022	1.382	1.456
4850626	RSBN1L	0.788	1.171	1.453
1470386	ASAH3L	1.334	1.483	1.452
3440692	SPRY4	1.042	1.355	1.452
3170450	IREB2	1.072	1.348	1.446
4290474	A930007F16RIK	0.919	1.292	1.441
2710494	F630038O13RIK	1.313	1.3	1.44
3390608	4732471D19RIK	0.929	1.316	1.44
670487	E430026H10RIK	1.263	1.347	1.437
460102	NUP50	1.064	1.277	1.436
1070450	RLBP1L1	1.481	1.396	1.435
4050292	B3GALNT2	1.183	1.42	1.434
1400047	4932415A06RIK	0.993	1.537	1.434
1430315	5830435K17RIK	2.101	1.472	1.431
3370575	RASGEF1B	1.289	1.188	1.43
520504	C730013O11RIK	0.979	1.113	1.429
2850719	HECW1	1.234	1.26	1.426
2630180	C130071E11RIK	0.896	1.216	1.426
6580239	SLMAP	1.123	1.405	1.424

620112	SALL3	1.061	1.257	1.421
7000241	RTN3	1.344	1.396	1.413
6560195	CLK4	1.307	1.407	1.411
4810307	ZFYVE16	1.087	1.499	1.408
70162	1810020C02RIK	1.262	1.472	1.404
6900369	HMG20A	0.944	0.864	1.404
650189	3632431M01RIK	1.089	1.211	1.402
380243	9530082I15RIK	1.146	1.285	1.4
3400014	SLK	1.119	1.4	1.4
4850066	B230310H07RIK	1.334	1.44	1.399
5670253	E2F3	1.17	1.243	1.399
3450053	PPP1R1C	0.946	1.237	1.397
5860736	B230339M05RIK	1.601	1.545	1.395
5890437	SNX13	1.152	1.338	1.392
840368	1700020I14RIK	0.996	1.26	1.392
6420435	PUS10	1.099	1.228	1.391
2370767	DOK5	1.057	1.145	1.39
2060487	SMEK2	1.13	1.229	1.39
160097	BMPER	1.178	1.207	1.39
3140241	TMED8	1.022	1.106	1.388
6510189	MTF1	1.623	1.3	1.386
7160132	A630082K20RIK	1.43	1.57	1.385
7160162	PSME4	1.296	1.618	1.384
2370575	ROCK2	1.384	1.593	1.383
4390722	D12ERTD551E	1.111	1.268	1.38
2600739	GPR85	0.831	1.112	1.375
6020300	ZFP449	1.305	1.24	1.374
6100465	TRPS1	1.182	1.368	1.371
4280338	WDHD1	1.021	1.213	1.371
2100243	KIF1B	1.21	1.394	1.371
1980470	ERO1LB	1.305	1.407	1.369
2030041	RANBP6	1.207	1.312	1.367
4200431	3222402P14RIK	0.95	1.183	1.366
4050612	FBXO11	1.228	1.404	1.366
6580703	RYR3	0.885	1.049	1.364
2480224	B230337C21RIK	1.14	1.393	1.364
1340270	CCNC	1.05	1.282	1.363
1070632	SPAG9	1.064	1.305	1.361
2070403	MTMR2	1.192	1.321	1.359
6510100	E330027P06RIK	1.171	1.385	1.359
6400634	TMEM47	1.007	1.232	1.359
7330324	MSL2L1	1.296	1.398	1.357
5270220	SH3BGRL2	1.069	1.43	1.356

5130431	AKAP11	1.099	1.05	1.356
3180097	HYAL1	1.161	1.226	1.353
1710735	LOC381219	1.198	1.322	1.353
6040753	MTUS1	1.064	1.15	1.353
7400747	CHD1	1.063	1.279	1.352
6980300	CRLF3	1.032	1.115	1.351
2480343	A430106G13RIK	1.264	1.426	1.35
1660564	NCKAP1	1.086	1.257	1.35
2850259	SYNE1	1.261	1.367	1.35
1470692	MLL3	1.028	1.102	1.349
6940093	6330444G18RIK	1.061	1.392	1.349
3060156	LOC100047794	1.018	1.197	1.348
2970292	GABRG3	1.247	1.327	1.347
7610386	CTTNBP2	1.06	1.262	1.346
4540020	DNAJB1	1.187	1.44	1.342
2100102	DGKI	1.119	1.081	1.341
240349	HECW1	1.163	1.333	1.341
4480494	4930487N19RIK	1.331	1.388	1.341
770181	9630009N10RIK	1.135	1.236	1.341
520286	PHXR4	1.073	1.437	1.34
4120669	LOC100046320	1.208	1.26	1.34
4060674	TACR3	1.061	1.16	1.34
5670026	4933432B09RIK	0.969	1.022	1.34
5550537	SLAIN2	1.038	1.295	1.34
6940706	CNTN5	1.126	1.112	1.34
5260176	NEO1	1.08	1.453	1.339
870079	E230027K01RIK	1.148	1.148	1.337
2750398	IPMK	1.246	1.339	1.336
6110546	OPA1	1.11	1.255	1.336
1170152	CLTC	1.097	1.373	1.335
1990446	NEURL	1.181	1.472	1.335
7330333	CYFIP2	1.086	1.055	1.335
3360059	SLC22A5	1.096	1.198	1.334
1780132	IMPACT	1.067	1.24	1.334
5820500	PDXDC1	1.345	1.18	1.332
4290722	ITGBL1	0.97	1.19	1.332
5960356	E430013K19RIK	1.277	1.332	1.331
6620195	TMEM135	1.025	1.1	1.33
4850102	A430103B12RIK	1.072	1.465	1.33
4290278	FOXC1	1.294	1.236	1.33
5820619	ZFP160	0.909	1.225	1.33
2470685	2610319H10RIK	1.083	1.305	1.329
1500382	SPAG9	1.038	1.17	1.328

3870730	A830054H12RIK	1.128	1.269	1.327
1110110	CDKL4	1.116	1.09	1.327
7510315	TRIM33	1.192	1.316	1.324
3370040	9330200H04RIK	1.327	1.277	1.323
2490092	AP2B1	1.064	1.288	1.323
7610403	LOC385058	1.118	1.344	1.323
3170451	ZSCAN20	1.062	1.382	1.322
3440465	RABEP1	1.058	1.332	1.322
7210255	ZFP654	1.126	1.383	1.322
7400044	FOSL2	1.604	1.441	1.321
5270195	P4HA1	1.313	1.457	1.32
1710280	LOC671523	1.007	1.191	1.32
4880008	ARL6IP2	1.35	1.292	1.32
2940487	PPM2C	1.218	1.303	1.318
2940136	BC018507	1.201	1.357	1.318
6520722	PBX1	0.935	1.164	1.316
870328	PTPN12	1.145	1.344	1.315
3840066	LIP1	1.127	1.281	1.315
3400328	PREI4	1.126	1.215	1.314
3850672	GPRK6	1.109	1.229	1.312
1660246	CPEB4	1	1.226	1.311
4060408	HMGCR	1.167	1.29	1.311
7100653	7420700D11RIK	1.289	1.371	1.311
2760059	TRIM33	1.088	1.204	1.31
4890674	FGFR2	1.21	1.022	1.31
4280121	D4ERTD681E	1.189	1.409	1.309
1940743	FN1	1.109	1.197	1.308
3850086	RIPK4	1.054	1.15	1.308
3130008	D730006F06RIK	0.967	1.185	1.307
4040382	LOC240672	1.324	1.352	1.307
1780707	9530053J19RIK	1.079	1.277	1.306
6520484	EIF4G2	1.26	1.455	1.305
1260719	KIFAP3	1.271	1.206	1.305
3520630	TGOLN1	1.303	1.386	1.304
3060682	SHPRH	1.154	1.248	1.304
2320390	B430201A12RIK	1.08	1.063	1.304
4230639	C130072A16RIK	1.255	1.283	1.304
7550685	HCFC2	1.157	1.315	1.304
2140671	ONECUT2	1.112	0.967	1.304
3130592	KBTBD8	1.067	1.141	1.303
2260358	LOC638935	1.199	1.24	1.303
2630451	9930115F03RIK	0.957	1.192	1.303
6760070	MIER1	0.988	1.059	1.303

4610669	ARHGAP18	0.906	1.32	1.302
6480554	BC023892	1.208	1.234	1.301
1440037	SLCO1A4	1.122	1.217	1.301
2490390	PLEKHA6	1.189	1.129	1.301
1850687	LOC100047837	1.266	1.111	1.301

Gene name	HSV-GFP cocaine	HSV-G9a cocaine
HSPA1A	1.754*	1.970
EGR2	1.927*	1.912
USP9X	1.179*	0.992#
PRKWNK3	1.256*	1.098#
FTSJ2	1.177*	1.137
TGFBR1	1.470*	1.033#
TNFRSF25	1.572*	0.959#
PER2	1.454*	1.413
ATM	1.341*	0.857#
ELMO1	1.463*	0.985#
CLK4	1.310*	1.233
RORB	1.226*	1.017
ΔFosB	3.520**	1.684#

*Represents a significant difference between repeated cocaine vs. saline treatment in HSV-GFP animals

Represents a significant difference between the effects of repeated cocaine in HSV-G9a vs. HSV-GFP animals

Table S4. Effect of G9a overexpression on genes that display increased mRNA induction in NAc following repeated cocaine. We randomly selected 12 genes from our microarray analyses that showed (at 1 hr) significant induction in NAc by repeated cocaine, but no induction by acute cocaine (Fig 1C; Tables S1 and S2). We then analyzed these genes in NAc of mice that received intra-NAc injections of HSV-GFP or HSV-G9a and were subsequently treated with repeated cocaine or saline. All 12 genes showed significant induction, in HSV-GFP injected animals, by repeated cocaine compared to saline treated controls. Out of these 12 genes, 6 genes (50%) displayed significant reductions in repeated cocaine-induced gene expression following G9a overexpression. In addition, we examined repeated cocaine induction of ΔFosB in NAc, which was also suppressed by G9a overexpression. Significance was determined using student's t tests comparing either HSV-GFP saline to HSV-GFP cocaine [(HSPA1A-t_9 = 2.676, *$p < 0.05$), (EGR2-t_9 = 2.975, *$p < 0.05$), (USP9X-t_9 = 2.406, *$p < 0.05$), (PRKWNK3-t_9 = 3.088, *$p < 0.05$), (FTSJ2-t_9 = 3.288, *$p < 0.05$), (TGFBR1-t_9 = 3.187, *$p < 0.05$), (TNFRSF25-t_9 = 1.840), (PER2-t_9 = 2.399, *$p < 0.05$), (ATM-t_9 = 2.164, *$p < 0.05$), (ELMO1-t_9 = 2.276, *$p < 0.05$), (CLK4-t_9 = 3.067, *$p < 0.05$), (RORB-t_9 = 1.962, *$p < 0.05$), (ΔFosB-t_8 = 6.064, *$p < 0.001$)] (*N = 5-6/group) or HSV-GFP cocaine to HSV-G9a cocaine [(HSPA1A-t_8 = 0.6916, $p > 0.05$), (EGR2-t_8 = 0.0315, $p > 0.05$), (USP9X-t_8 = 2.992, $^{\#}p < 0.05$), (PRKWNK3-t_8 = 1.809, $^{\#}p \leq 0.05$), (FTSJ2-t_8 = 0.5742, $p > 0.05$), (TGFBR1-t_8 = 2.828, $^{\#}p < 0.05$), (TNFRS25-t_8 = 1.975, $^{\#}p < 0.05$), (PER2-t_8 = 0.1852, $p > 0.05$), (ATM-t_8 = 3.154, $^{\#}p < 0.05$), (ELMO1-t_8 = 2.202, $^{\#}p < 0.05$), (CLK4-t_8 = 0.6397, $p > 0.05$), (RORB-t_8 = 1.593, $p > 0.05$), (ΔFosB-t_7 = 4.317, $^{\#}p < 0.05$)] ($^{\#}$N = 4-

6/group). Viral data are presented as the mean relative fold change from HSV-GFP saline controls.

Table S5. Complete Primer List

Mouse mRNA Primers

GAPDH-F	AGGTCGGTGTGAACGGATTTG
GAPDH-R	TGTAGACCATGTAGTTGAGGTCA
G9a-F	TGCCTATGTGGTCAGCTCAG
G9a-R	GGTTCTTGCAGCTTCTCCAG
GLP-F	ATTGACGCTCGGTTCTATGG
GLP-R	ACACTTGGAAGACCCACACC
Suv39H1-F	CTGTGCCGACTAGCCAAGC
Suv39H1-R	ATACCCACGCCACTTAACCAG
Suv39H2-F	GCTGTGGTTGGGGTGTAAAA
Suv39H2-R	GCTGCATCCACTGTGAACTC
SETDB1-F	GATTCTGGGCAAGAAGAGGA
SETDB1-R	GTACTTGGCCACCACTCGAC
EZH2-F	TTTGCTGCTGCTCTTACTGC
EZH2-R	CCAGTTTCAGTCCCTGCTTC
JmjD2A-F	GACTCACCACCGAGACCTTC
JmjD2A-R	GATGTCCCAGACCCAAAGTG
JmjD2B-F	AGCGATGGAAACTGAAATGC
JmjD2B-R	ACCACATAGGGCCAGTCATC
JmjD2C-F	GGCTCCTTCAGCAGAGACAC
JmjD2C-R	GGCCATTTGACTTGGATGAC
LSD1-F	ACGCCACACCTCTCTCTACC
LSD1-R	CACAGCAATCACTTCACATCC
JMJD3-F	CACTTCGGCTCAACTTAGGC
JMJD3-R	GTCCCAGTTCTCGTCTGAGG
UTX-F	TAAATGTCCGCCTCCAAGAC
UTX-R	AACAGGGTTGTTTGGGTTTG
HSPA1A-F	CAAGATCACCATCACCAACG
HSPA1A-R	ATGACCTCCTGGCACTTGTC
EGR2-F	GAAGGAACGGAAGAGCAGTG
EGR2-R	AGCCAGAGCTTCATCTCACG
USP9X-F	TGGCATGATTGCTCTATTGAAG
USP9X-R	TCGGTAGGTGGAGGGTTTAG
PRKWNK3-F	AAGCTGGTGGATGACTGGAC
PRKWNK3-R	CCATGAAATGAAGGGAGTGG
FTSJ2-F	GCAAAGGTGGAGAGTTACCG
FTSJ2-R	ACAGGAGAGCTGGAATCTGC
TGFBR1-F	TCTGCATTGCACTTATGCTGA
TGFBR1-R	AAAGGGCGATCTAGTGATGGA
TNFRSF25-F	CCGGGAGAAGAGGGATAGCTT
TNFRSF25-R	TGGACAGTCACTCACCAAGT

PER2-F	GAAAGCTGTCACCACCATAGAA
PER2-R	AACTCGCACTTCCTTTTCAGG
ATM-F	GATCTGCTCATTTGCTGCCG
ATM-R	GTGTGGTGGCTGATACATTTGAT
ELMO1-F	TGTATTTCGCTAAGCACCACC
ELMO1-R	CCATACGACACTGGCAGTATCT
CLK4-F	ATGCGGCATTCCAAACGAAC
CLK4-R	GTACTGCTGTGAGACCTTCTCT
RORB-F	GCAGCATTAGCAATGGCCTC
RORB-R	GACGGCTGACCGGAATCTATG
ΔFosB-F	AGGCAGAGCTGGAGTCGGAGAT
ΔFosB-R	GCCGAGGACTTGAACTTCACTCG

Human mRNA Primers

G9a-F	CATTTCCGCATGAGTGATGATGT
G9a-R	GGCAGAACCTAACTCCTCCGA

Rat mRNA Primers

G9a-F	GACAACAAGGATGGTGAGGTC
G9a-R	AGCATGAAGACCCGAACAG

Mouse Promoter Primers

Cdk5-F	AACACCCAACCAGGTCAGAG
Cdk5-R	CGCGTTCCAGAATACAGTGA
p65/Rel-A-F	GGTTCCGGAGATCCCTAAAG
p65/Rel-A-R	AGAGTCCCTGAGAGCCATGA
Arc-F	AGGTTGGGCAGGAAGTAGGT
Arc-R	CCTCAGCTGCCTTTGGTTAG
FosB-F	GGAGGTTTGTGCATGGAGTT
FosB-R	AGCCGCTCCAGTCTTATGAA
LIMK-F	CCTTCCGCTGTTCACAGACT
LIMK-R	CTCTCCAGGCCAGTTTAGGG
BDNF IV-F	CTTCTGTGTGCGTGAATTTGCT
BDNF IV-R	AGTCCACGAGAGGCTCCA
cFos-F	TCCCTCCCTCCTTTACACAG
cFos-R	CCCGTCTTGGCATACATCTT
APRT-F	TGCTGTTCAGGTGCGGTCAC
APRT-R	AGATCCCCGAGGCTGCCTAC

Supporting References and Notes

S1. S. J. Russo *et al.*, *J Neurosci* **29**, 3529 (2009).
S2. S. C. Sampath *et al.*, *Mol Cell* **27**, 596 (2007).
S3. B. Y. Ahmed *et al.*, *BMC Neurosci.* **5**, 4 (2004).
S4. T. E. Scammell *et al.*, *J. Neurosci.* **23**, 5762 (2003).
S5. M. B. Kelz *et al.*, *Nature* **401**, 272 (1999).
S6. L. I. Perrotti *et al.*, *J. Neurosci.* **24**, 10594 (2004).
S7. W. Renthal *et al.*, *Neuron* **56**, 517 (2007).
S8. Q. LaPlant *et al.*, *Biol Psychiatry* **65**, 874 (2009).
S9. X. Peng *et al.*, *BMC Bioinformatics* **4**, 26 (2003).
S10. L. Shi *et al.*, *Nat Biotechnol* **24**, 1151 (2006).
S11. L. Guo *et al.*, *Nat Biotechnol* **24**, 1162 (2006).
12. O. Berton *et al.*, *Science* **311**, 864 (2006).
S13. J. D. Hommel, R. M. Sears, D. Georgescu, D. L. Simmons, R. J. DiLeone, *Nat. Med.* **9**, 1539 (2003).
S14. J. H. Han *et al.*, *Science* **323**, 1492 (2009).
S15. M. Ellgren, S. M. Spano, Y. L. Hurd, *Neuropsychopharmacology* **32**, 607 (2007).
S16. M. S. Spano, M. Ellgren, X. Wang, Y. L. Hurd, *Biol Psychiatry* **61**, 554 (2007).
S17. W. Renthal *et al.*, *Neuron* **62**, 335 (2009).
S18. T. I. Lee, S. E. Johnstone, R. A. Young, *Nat Protoc* **1**, 729 (2006).
S19 M. Barrot *et al.*, *Proc Natl Acad Sci U S A* **99**, 11435 (2002).

Supporting Online Material

www.sciencemag.org

Materials and Methods
Supporting Text: Detailed Figure Legends Including Statistics
Supporting Figures (Fig. S1-S8) and Tables (Table S1-S5)
Supporting References and Notes